WSRC-TR-2002-00253
June 10, 2002

Cesium-137 in the Sediments of Fourmile Creek (U)

D.M. Beals, K.J. Hofstetter and L.S. Nichols
Savannah River Technology Center
Westinghouse Savannah River Co.
Aiken SC 29808

This document was prepared in conjunction with work accomplished under Contract No. DE-AC09-96SR18500 with the U. S. Department of Energy.

Table of Contents

List of Figures

List of Tables

List of Photos

List of Appendices

List of Acronyms and Abbreviations

4MC	Fourmile Creek (a.k.a. Fourmile Branch)
cps	counts per second
ER	Environmental Restoration Division
FMB	Fourmile Branch (a.k.a. 4MC)
HPGe	High Purity Germanium γ-ray Spectrometer
IOU	Integrator Operable Unit
μR/h	radioactive dose in micro-rem per hour
NaI(T*l*)	Sodium Iodide Scintillation γ-ray Spectrometer
NTS	Nonproliferation Technology Section
pCi/g	picoCuries per gram of radioactivity
SRS	Savannah River Site
SRTC	Savannah River Technology Center

Executive Summary

The inventory of ^{137}Cs remaining in the Fourmile Creek floodplain has been estimated using aerial and ground γ-ray spectrometry data. Methods were developed to convert *in-situ* measured counts per second in the ^{137}Cs photopeak to pCi/g of ^{137}Cs in the sediment taking into account the average soil density and the depth of the contamination. In areas where *in-situ* measurements were not made, the EG&G aerial overflight results were used to estimate the inventory of ^{137}Cs. As of 2001, the decay-corrected inventory released to the creek was 28 Curies, of which at least 72% was expected to be deposited to the sediments. The total inventory of ^{137}Cs in the Fourmile Creek floodplain based on this study is estimated to be 23 Curies.

Introduction

The Nonproliferation Technology Section (NTS) was requested by the Environmental Restoration Division (ER) to aid in completing ground-truth measurements of aerial overflight data in support of the Integrator Operable Unit (IOU) program at the Savannah River Site (SRS). The IOU's at the SRS are under investigation as a possible pathway for the release of contamination from past SRS activities to off-unit receptors and the environment. The IOU's are defined as surface water bodies and associated wetlands, including the water, sediment and related biota. The objective of the IOU program is to: assess the risk to potential human and ecological receptors from IOU contamination; evaluate the impact of inactive and active waste units and operating facilities on the IOU quality; determine if IOU early actions, including reprioritization of operable units implementation schedules, are necessary; and complete the remedial investigation/feasibility study process, defining the nature and extent of IOU contamination, remedial action objectives, and final remediation goals.

Aerial surveys are periodically completed at sites of interest to the Department of Energy, such as the SRS, to document baseline radiological conditions. A high performance helicopter equipped with two complete radiation detector and data acquisition systems is used for the aerial survey **[1]**. The radiation detector systems contain NaI(T*l*) scintillation detectors. The gross counting rate measured by the radiation detectors is later converted to an exposure rate in μR/h assuming a uniformly distributed source covering an area which is large when compared to the detector's field of view (~100m diameter at 46m altitude). The products of the surveys have been integrated onto site maps depicting the distribution of the radioisotope of interest with isopleths used to indicate different areas of activity. These surveys demonstrated that the major isotope remaining on the 800-km^2 site is ^{137}Cs, confined primarily to the stream channels.

The NTS was asked to assist ER in ground-truthing the aerial overflight data using its portable γ-ray survey equipment. The initial study encompassed the Steel Creek watershed **[2,3]**, an area comprising ~91-km^2 in the south central portion of the SRS. This report details the work completed in the Fourmile Creek (4MC) watershed. The 4MC watershed is an area of ~57-km^2 in the western part of the SRS which empties into the Savannah River. Fourmile Creek receives effluents from the seepage basins of two chemical separation facilities (capped in 1990), liquid and solid waste disposal facilities and, until 1985, cooling water from one of the production reactors at SRS. From facility effluent data, the total decay-corrected inventory of ^{137}Cs released to Fourmile Creek from site operations was estimated to be ~28 Ci as of 2001 **[4]**. Using data collected in 1978, Chen **[5]** recently modeled that as much as 72% of the cesium introduced to the 4MC would be deposited to the sediments.

The following sections describe the field portable γ-ray spectrometers used to measure the radioactivity in the sediments along the 4MC floodplain, and then the models developed to convert *in-situ* measured counts per second in the ^{137}Cs photopeak to pCi/g of ^{137}Cs in the sediment, taking into account the average soil density and the depth of the contamination **[6]**. This information was then coupled with the aerial overflight data to calculate the inventory of ^{137}Cs remaining in the 4MC floodplain **[7]**. The results from all the field measurements are included in the Appendix to this document.

Methods of Analysis

The results of the most recent aerial surveys (1991 **[1]** and 1998 **[8]**) were used to identify sampling transects for surface radiation measurements along the 4MC. Thirteen transects were selected along the creek (transects 4-16); an additional three transects (transects 1-3) were established in the Savannah River swamp area near the discharge of 4MC into the Savannah River floodplain (Figure 2 and 1, respectively). All transects were chosen by ER based on the count rates observed in the 662 keV region of the spectrum recorded in the aerial surveys. Most transects were made perpendicular to the stream flow and went from near the headwaters of the creek, near the discharge locations, to the floodplain of the Savannah River. They extended from areas of background through the areas of the highest ^{137}Cs count rates and back to background on the opposite bank. Several transects were made parallel to the stream channel through areas of increased activity based on the aerial survey data.

Figure 1. Locations of Transects 1-3 in Fourmile Creek

Figure 2. Locations of Transects 4-16 in Fourmile Creek

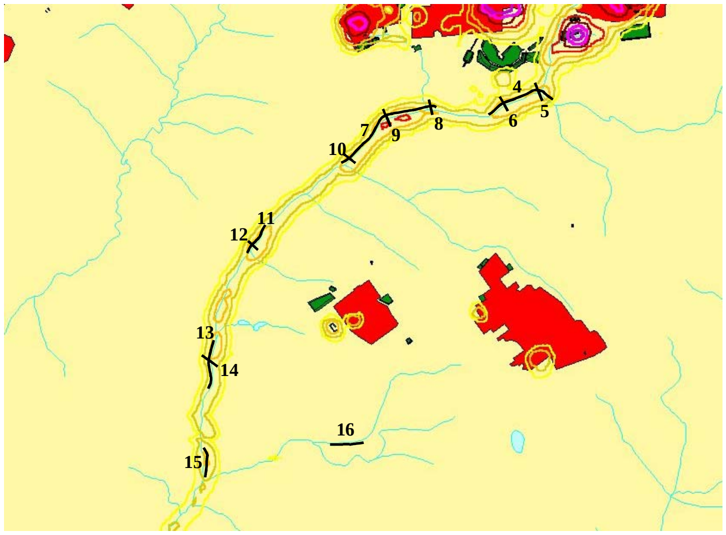

After clearing the selected transects, the precise measurement locations were determined using a differentially corrected geographic positioning system (GPS) and field survey equipment. The field measurements made by the NTS were performed at ~60 meter intervals in background areas and at ~30 meter intervals in areas of higher ^{137}Cs levels along each transect. The field measurements were made using the Berkley Nucleonics Corp. (BNC) Survey and Monitoring (SAM) 935 analyzer. The SAM 935 consists of a 5-cm x 5-cm NaI(T*l*) detector coupled to a multi-channel analyzer. The detector was placed in a tripod and held 30 cm above the ground (Photo 1). A three-minute spectrum was recorded at each location. A second measurement was made at each location with a 5-cm thick lead absorber placed directly below the detector to determine the surrounding background. The total net count rate (0-2000 keV) and the count rate in the ^{137}Cs photopeak (662 keV) were determined in each spectrum. The average peak intensity in the soil directly under the detector (radius ~25 cm) was determined by subtracting the shielded count rate from the unshielded count rate at each location.

For the original Steel Creek survey work **[2,3]** Microshield™ [1] was used to estimate the soil concentration (pCi/g) of ^{137}Cs which would yield the observed net peak intensity at each measured location. Modeling the source spatial and depth distribution utilized a source configuration developed from soil compositions described by Miller and Shebell **[9].** The model assumed a uniform source distribution of ^{137}Cs in the top 0.5 cm of soil with a bulk density of 1.6 g/cm^3. Moisture content was assumed to be 10% at all sampling locations. Surface soil samples had been collected from 28 of the 131 *in-situ* measurement locations. These were returned to the lab and analyzed by high-resolution γ-ray spectroscopy using a high purity germanium (HPGe) detector. A correlation coefficient of $r^2 = 0.71$ (Figure 3) was found between the field survey results calculated by Microshield™ and the laboratory results. Of the 18 samples collected that had ^{137}Cs in excess of the Site benchmark value (21.8 pCi/g), 16 were found using the field survey

[1] Microshield™ Version 4.0, Copyright 1987, Grove Engineering, Rockville MD

Photo 1. SAM 935 Deployed in the Field

Figure 3. Correlation Between Lab HPGe and Field NaI(T*l*) Results

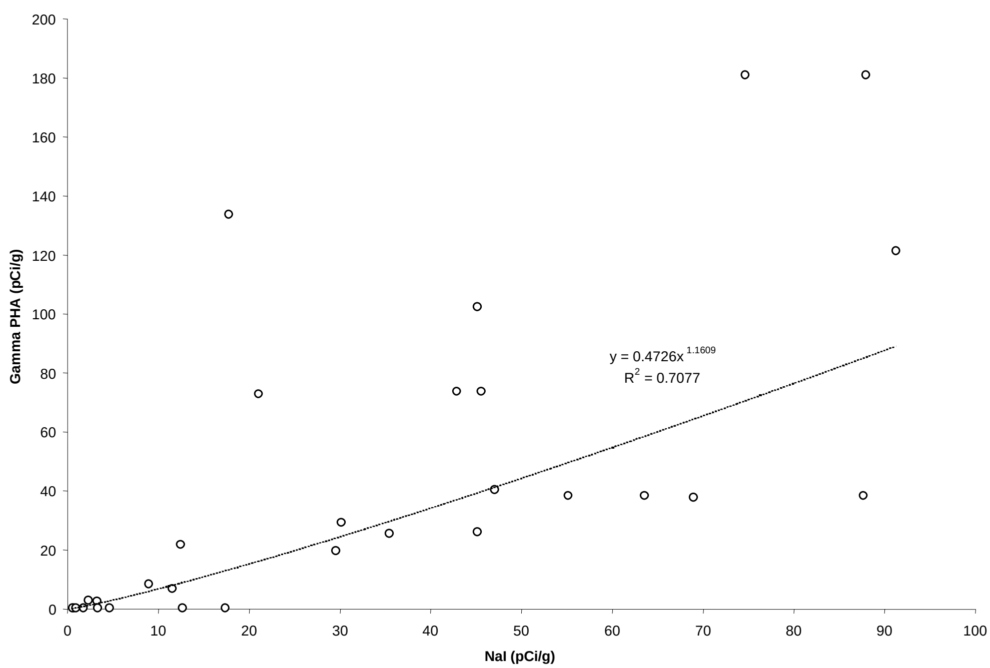

method. This demonstrated the usefulness of the field measurement technique thus ER requested that the NTS participate in surveying the remaining streams on the SRS.

When converting the field **γ**-ray count rates to activity in the soil for the Steel Creek work, the Microshield™ model used assumed that the ^{137}Cs was uniformly distributed in the top 0.5 cm of the soil. Literature suggested the depth distribution of the ^{137}Cs in soil is probably exponential **[10]** but due to reduced operations at the SRS it was suspected that there might be a considerable clean earth overburden in some locations. To better understand the depth distribution of the ^{137}Cs in the 4MC floodplain a series of core bore samples were taken. The total net count rates (0-2000 keV) were used to select locations for the core bore sampling. Segmented core-bore samples were taken at these locations and composited into 0-1 foot, 1-3 foot and 3-5 foot sub-samples. Typically one core-bore was taken per transect. These composites were taken to the laboratory for detailed γ-ray spectrometry analyses using a HPGe detector.

After removal of the core-bore samples, the resulting holes were surveyed by the NTS. A 2.5-cm x 2.5-cm NaI(T*l*) detector was coupled to a SCOUT portable multi-channel analyzer (Photo 4). A 5-cm by 60-cm long plastic pipe was inserted into the hole left by the core bore operation (Photo 2). The NaI(T*l*) probe was then lowered into the plastic pipe (Photo 3) and spectra recorded every 5 cm. A 3-cm thick Bi/Sn alloy absorber (density 8.7 g/cm^3) was placed over the end of the detector to reduce the detection of activity in the axial direction. The net count rate in the ^{137}Cs photopeak was then used to determine the relative depth distribution of the ^{137}Cs activity at 5-cm intervals.

Photo 2. Inserting the Pipe into the Bore Hole

Photo 3. SCOUT Detector in the Bore Hole (mid-depth)

Photo 4. SCOUT Detector in Bore Hole (at bottom of hole)

Results

The results from each transect are shown in the Appendices. One figure in each appendix shows the gross count rates for the unshielded detector, the background rate from the shielded detector, and the residual count rate from the ground measurement along the transect. The lines are a smoothed spline fit to the data and merely added as a visual aid. The 1991 aerial survey data (corrected to count rates expected at one meter above the ground) were within the same general range of count rates measured by the unshielded NaI(T*l*) detector. The next figure shows the net count rates at these same locations in the 662 keV region of the spectrum. The detection limits are based on the method described by Currie **[11]** at the 95% confidence level. The error bars on the count rates are reported at the 2-sigma level. The increased count rate for the ^{137}Cs photopeak coincides with the increased residual count rate (0-2000 keV) suggesting that ^{137}Cs is the primary contributor in the spectra. No other **γ**-rays from man-made radionuclides were evident in any of the field spectra.

The next figures in the appendix show the count rates for the full spectrum (0-2000 keV), and for the 662 keV (^{137}Cs) photopeak as observed in the spectra taken with the down-hole NaI(T*l*) probe, if completed. As before, the error bars are shown at the 2-sigma level. No other man-made radionuclides were evident in the down-hole spectra.

Model Development

Several computer codes in combination with laboratory calibrations were used to generate the response function of the 5-cm by 5-cm NaI(T*l*) detector used for the ground surface measurements in the field. Using the dual spectrum/absorber measurement technique, the effective area samples with the detector was calculated to be ~2000 cm^2.

Figure 4. Count Rate Generated with ^{137}Cs Source

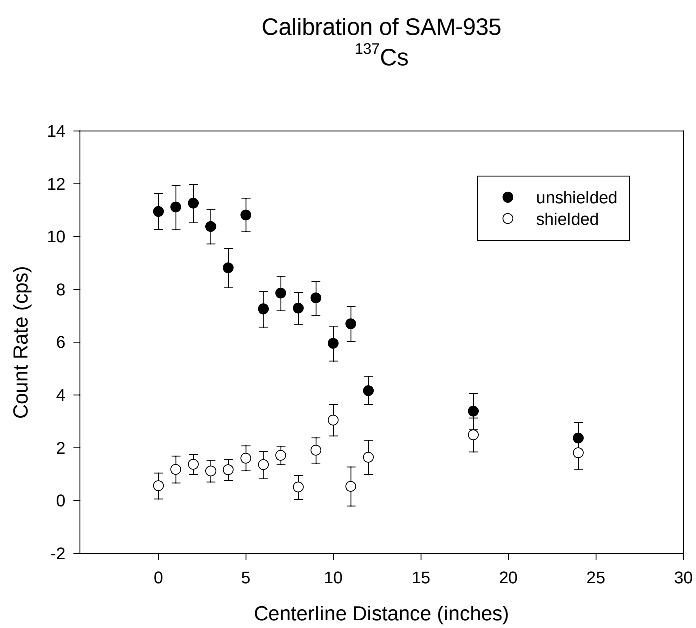

This was confirmed in the laboratory using a point source located 30 cm from the detector face and moved radially outward from the detector centerline (Figure 4). The detection efficiency and peak-to-total ratio was measured for the detector at this distance using a calibrated ^{137}Cs source. The measured detection efficiency for the 662 keV photopeak at 30 cm was used to benchmark all the computer code simulations.

Microshield™ was the first code used to estimate the soil concentrations of ^{137}Cs. This code computes the average dose rates observed for various extended source configurations. The SAM 935 field instrument was calibrated by the manufacturer to calculate the dose rate contributions for individual radionuclides and read out the total dose rate based on the actual spectrum. In most cases ^{137}Cs was the primary dose contributor to the spectra. The fluxes of γ-rays reaching the detector for various extended source configurations were also output from Microshield™ and compared to the observed 662 keV net peak intensity at each measured location. As stated previously, the model assumed a uniform source distribution of ^{137}Cs in the top 0.5 cm of the soil. Based on the bore-hole surveys, the average depth of peak activity was ~10 cm, with less contaminated overburden overlying the peak, as predicted above based on Site activities.

Figure 5. Count rates for ^{137}Cs (1 pCi/gm) in 5 cm layer of contaminated soil with density = 1.6 gm/cm^3

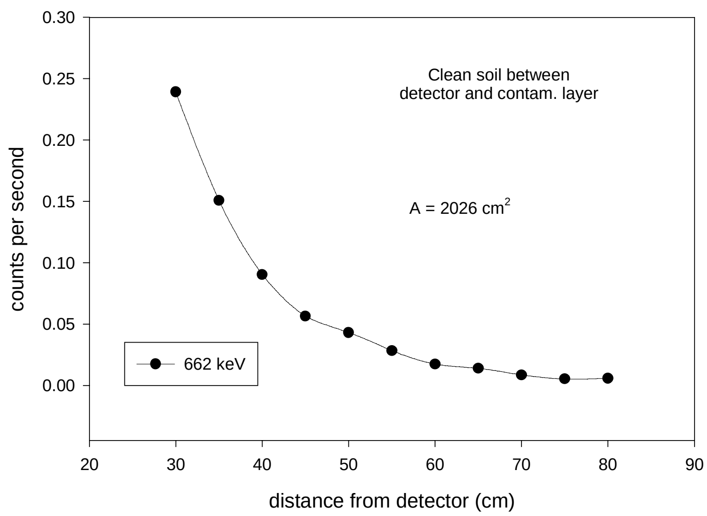

To incorporate the measured depth distribution the computer codes SYNTH[2] and ETNA[3] were used to simulate spectra for various source configurations. SYNTH was used to model the source conditions at a source-to-detector distance of 30 cm. ETNA was used to transform the point source calibrations for the NaI(T*l*) detector to extended source geometries. To reflect the depth distribution measurements, source distributions were

[2] SYNTH, W.K. Hensley, et al. Pacific Northwest National Lab
[3] ETNA, Marie-Christine Lepy, et al. Laboratoire National Henri Becquerel, CEA/Saclay

calculated as 5-cm thick segments of 2000 cm^2 area. The ^{137}Cs was assumed to be uniformly distributed throughout the disk. As before, the matrix was assumed to be soil of composition suggested by Miller and Shebell **[9]**. Calculations were then repeated for photopeak intensities at 30 cm as the disks were overburdened with clean soil of the same elemental composition in 5-cm increments. The results of this calculation are shown in Figure 5 and indicate that the intensity of the transmitted γ-rays at 662 keV falls off dramatically as the thickness of the uncontaminated soil increases. To check the consistency of the calculations, the count rates observed at 30 cm for a source of various thicknesses were calculated and are shown in Figure 6. The result of this calculation shows the mean-free path for the 662 keV γ-ray in soil is ~30 cm, which is consistent with reported values **[10]**.

Figure 6. Count rates for ^{137}Cs (1 pCi/gm) uniformly distributed in soil with density = 1.6 gm/cm^3

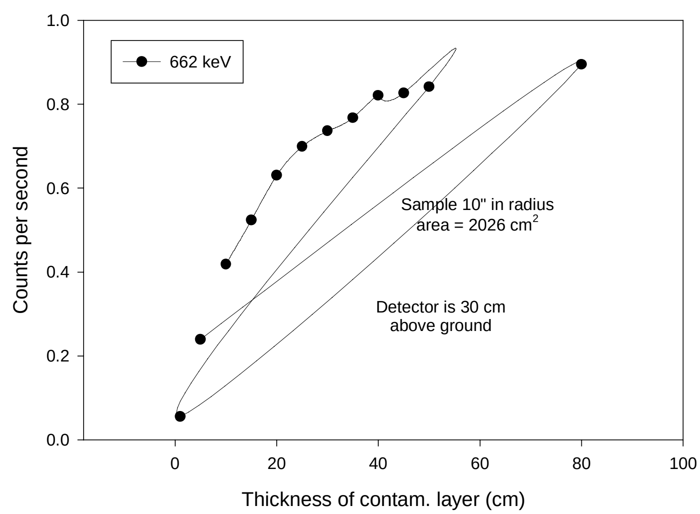

The response of the surface detector to ^{137}Cs for various depth distributions could then be calculated from the measured field depth profiles and the recorded surface count rates using the following:

$$CR = \Sigma f_i * C_i$$

where CR is the calculated count rate for a uniformly distributed source of 1 pCi/g in soil of density 1.6 g/cm^3 in a measured depth distribution containing f_i fraction of counts in the i^{th} interval. C_i is the calculated count rate for the 662 keV γ-ray in the i^{th} interval for a 1 pCi/g source. The intervals represent the 5 cm depth increments. As an example of this calculation see the following table (Table 1) taken from Appendix C (transect 3).

The first column gives the distance to the top of a 5-cm layer of contaminated soil to the detector. The second column is the thickness of the clean soil layer on top of the ^{137}Cs

contaminated layer. The third column is the result of the SYNTH calculation for the 662 keV γ-ray for a single 5-cm thick layer of soil contaminated to 1 pCi/g ^{137}Cs at various depths (Figure 5). The next column is the observed count rate for the downhole probe as a function of distance down the corebore hole (Figure 7 from [Appendix 3]). The fraction of events observed at each location is shown in the fifth column. The last column is the result of the product calculation of the intensity (column 3) times the fraction of events occurring at that location (column 5) using the model predictions. Summing the last column gives the overall count rate (0.086 cps) at 30 cm observed for a 1 pCi/g ^{137}Cs source distributed throughout the soil as determined by the depth profile. Dividing the observed count rate at 30 cm above the surface by this calculated count rate gives the estimated ^{137}Cs content in pCi/g at that location. The calculated ^{137}Cs activity at each field measurement location is provided in each Appendix.

Figure 7. ^{137}Cs Count Rate in Bore Hole FMB 03-02

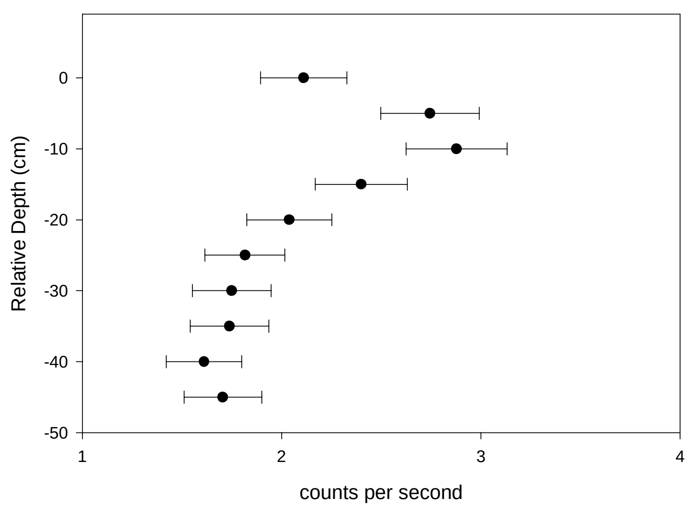

Table 1. Calculated Conversion Rate to Convert Field cps to pCi/g ^{137}Cs

distance to detector cm	soil absorber cm	SYNTH count rate cps	observed count rate cps	fraction	product
30	0	0.2392	2.1	0.121	0.029
35	5	0.1507	2.7	0.157	0.024
40	10	0.0904	2.9	0.165	0.015
45	15	0.0564	2.4	0.137	0.008
50	20	0.04295	2.0	0.117	0.005
55	25	0.02825	1.8	0.104	0.003
60	30	0.01725	1.8	0.100	0.002
65	35	0.01385	1.7	0.099	0.001
		total=	17.5	sum=	0.086

Calculation of ^{137}Cs Inventory

The results of the field measurements and the aerial γ-ray distribution measurements were geo-registered onto SRS site maps using standard GIS techniques which uses ArcView® to analyze and display data. ArcView® was used to plot the field survey data over the radiological isopleths determined from the aerial surveys, which covered the entire watershed. Combining the calculated field sample results with the ^{137}Cs distribution, determined by the aerial surveys, permitted an estimate of the ^{137}Cs inventory. A description of the process used to combine the field and model data in order to estimate the total inventory of ^{137}Cs within the 4MC floodplain follows.

Transects 7-10 (Figure 8) are near the discharge of the seepage basins from one of the chemical processing facilities into 4MC. Transects 8, 9 and 10 are approximately 280 meters long and run perpendicular to the creek at successive downstream locations (~800 meters apart). Transect 7 runs the length of the creek between transects 8 and 10. The measurements along transect 7 were within 10 m of the creek channel. The total length of transect 7 measured in ArcView® was 1453 m. Transects 8, 9, and 10 showed that the ^{137}Cs contamination extended 50 m on either side of the creek channel (Appendix H, I, J). This gives a width of 100 m for the contaminated floodplain. The bore hole measurements showed the depth of contaminant to be ~ 10 cm (0.10 m, Appendix G). Using these values, the total volume occupied by the contaminant was determined. Multiplying by the average soil density, 1.6 g/cm^3, gave the total grams of contaminated soil.

Figure 8. Locations of Transects 7-10 on Fourmile Creek

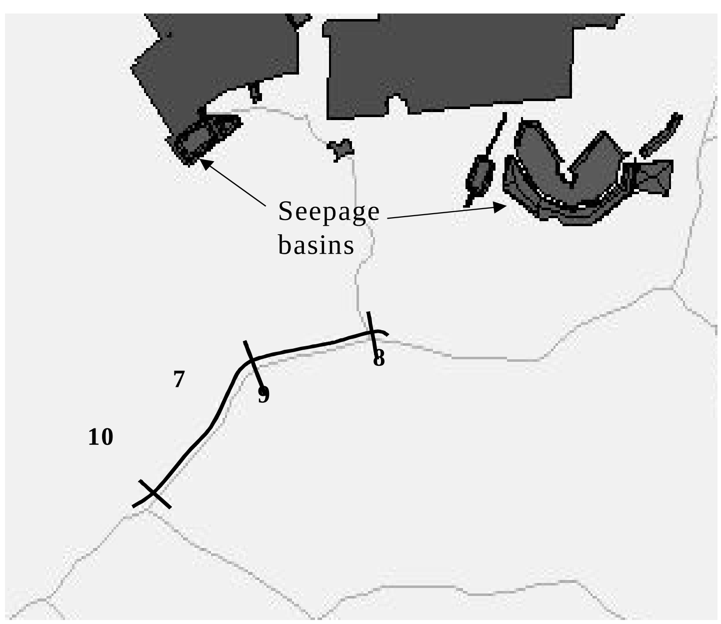

Table 2. Values used in Calculating the Inventory of ^{137}Cs in the Fourmile Creek Floodplain

Region	length (m)	width (m)	Average observed count rate (cps) *	Calculated count rate (cps per pCi/g) *	Inventory of ^{137}Cs (Curies)
headwater to transect 4	250[a]	200	10	0.08	1.0
	255[b]	115	0.5	0.08	0.03
transects 4-6	800	75	**6.7**	0.08	0.71
between transects 4 & 7	816[b]	150	0.5	0.08	0.12
transects 7-10	1453	100	**15.8**	**0.078**	4.71
between transects 7& 11	1200[b]	150	0.5	0.075	0.19
transects 11-12	600	75	**17.9**	**0.072**	1.79
between transects 11 & 13	370[a]	100	10	0.07	0.85
	580[b]	150	0.5	0.07	0.10
transects 13-14	470	100	**5.3**	0.06	0.66
between transects 13 & 15	885[b]	150	0.5	0.06	0.18
	85[c]	200	ND		
transect 15	500	40	**6.1**	**0.059**	0.33
transect 15 to transect 1	3383[b]	100	0.5	0.053	0.51
	4444[c]		ND		
	793[d]		ND		
	947[c]	200	ND		
transect 16	254	100	**<0.6**		
above transect 1	300[b]	600	**1.6**	**0.047**	0.98
between transects 1 & 2	900[c]	1300	1.5	0.052	5.4
hot spot on 2	250[a]	320	**4.3**	**0.057**	0.97
between transects 2 & 3	900[b]	1500	1.2	0.072	3.6
hot spot on 3	85[a]	200	**2.3**	**0.086**	0.01
transect 3 to river	120[b]	230	**0.9**	0.086	0.05
	730[b]	600	**0.9**	0.086	0.73
	700[b]	250	**0.9**	0.086	0.29
	1500[c]	600	**<0.6**		
TOTAL					**23.2**

[a] distances located within the 914-cps isopleth from aerial survey data
[b] distances located within the 286-cps isopleth from aerial survey data
[c] distances located within the 91-cps isopleth from aerial survey data
[d] distances located within the background cps from aerial survey data
* numbers in **bold** were obtained from field measurements

The observed ^{137}Cs count rate was averaged over transect 7 and resulted in a mean count rate of 15.8 cps (refer to Appendix G). This value was then divided by the calculated ^{137}Cs count rate obtained from the simplified model (0.078 cps per pCi/g, Appendix G) to obtain the activity of ^{137}Cs per gram of sediment within the area. Multiplying the activity of ^{137}Cs by the total mass gives the inventory of ^{137}Cs in that area. For the area covered by transects 7-10 a total of 4.7 Ci of ^{137}Cs is estimated to be present. The above process was repeated for the areas along transect 4, 11, 13, 15, and 16 and in the swamp (transects 1-3). Results are shown in Table 2. Width of ^{137}Cs contamination was determined using the field measurements for transects traversing the creek whenever available, otherwise, the width of the isopleth, as determined from the aerial surveys. Along the transects, the count rate is the average of the cps for the ^{137}Cs photopeak determined by the surface γ-ray measurements.

Between the transects along the main channel of the creek, prior to the swamp, the average count rate was determined by the aerial isopleth data compared to the areas in which measurements were made. Transects 4, 7 and 11 were all located within the 914-cps isopleth. The average count rate along all these transects is about 10 cps, thus in areas within the 914-cps isopleth a value of 10 cps was assigned when not directly measured. This occurred above transect 4 and between transect 11 and 13. Surface measurements made within the 286-cps isopleth averaged 0.5 counts per second thus this value was used for all areas not directly measured. The few surface measurements made within the 91-cps isopleth had no detectable ^{137}Cs photopeak, thus were assigned a value of "non-detectable."

In the swamp two "hot-spots" (indicated by the 914-cps isopleth) were noted on the aerial surveys, one each on transects 2 and 3. The average measured count rate was 4.6 and 2.3 cps, respectively. The average count rate along transect 1 was about 1.6 cps; this value was used to calculate the ^{137}Cs inventory within the isopleths above transect 1. Excluding the "hot-spot" on transect 2, the average count rate was 1.4 cps. This was averaged with the transect 1 value (1.6) and used to calculate the inventory between transect 1 and 2. Similarly, the average count rate on transect 3 (excluding the "hot-spot) was averaged with the transect 2 average to calculate the inventory between transect 2 and 3. The transect 3 average was used to estimate the inventory within the 286-cps isopleth below transect 3; the 91-cps isopleth below transect 3 was non-detectable by the field measurement system.

The factor to convert the surface cps to pCi/g (column 5 in Table 2) for transect 7 was used to calculate the inventory from the headwaters, through transect 4 to transect 7. Between transect 7 and 11 the average conversion factor was used. Discharges from the C-reactor entered 4MC immediately above transect 13 and had scoured a deep channel while the reactor was operating. More sedimentation has since occurred in this part of the 4MC, depositing cleaner sediment over the^{137}Cs contaminant peak. This has reduced the surface measured count rate, resulting in a lower detection efficiency (smaller conversion factor). Because the same process is occurring along transect 13 and 15, the conversion factor calculated for transect 15 was used for transect 13, and all areas below transect 13. The average value of transect 15 and transect 1 was used to convert the cps to pCi/g of ^{137}Cs between these areas. In the swamp region the conversion factor increases with distance into the swamp, implying less fresh, clean, sediment being deposited further into the swamp. The average of transect 1 and 2 was used to calculate the inventory between those transects, and the average of 2 and 3 to calculate the inventory in that region. The conversion determined for transect 3 was used for all areas below transect 3.

Conclusions

In-situ ground surface radiation measurements were made along predetermined transects within the Fourmile Creek Watershed on the SRS. The field measurements were coupled with previously analyzed aerial γ-ray surveys to determine the amount of ^{137}Cs remaining within the 4MC floodplain. A total inventory of ~23 Ci of ^{137}Cs was calculated to remain in the sediment of the floodplain, divided about evenly between the upper creek and the swamp. This value is in reasonable agreement with the total decay-corrected inventory of ~28 Ci of ^{137}Cs released to the 4MC.

Acknowledgements

The authors wish to thank Ron Johnson, Wanda Matthews and Sandra Nappier for support in completing the field surveys and Kane Bice and Eric Barron for support in siting and clearing the transects. This work was performed under the auspices of the US Department of Energy by the Savannah River Technology Center under contract no. DE-AC09-96SR18500.

References

[1] R. J. Vojtech, "An Aerial Radiological Survey of the Savannah River Site and Surrounding Area October-November 1991," *EG&G Report,* 11265-1236 (1993).

[2] K. J. Hofstetter, D. M. Beals, G. A. McLane, T. K. Honeycutt and L. S. Nichols, "*In-Situ* Measurements of ^{137}Cs in the Steel Creek Watershed at SRS," *ANS Transactions*, **81**, 133-135 (2001).

[3] K.J. Hofstetter, "Cesium-137 in the Steel Creek Watershed," in preparation.

[4] W. H. Carlton, L. R. Bauer, L. A. Geary, C. E. Murphy, Jr., J. E. Pinder, and R. N. Strom, "Cesium in the Savannah River Site Environment," *SRS Report WSRC-RP-92-250*, March (1992).

[5] K-F. Chen, "Modeling the Transport of Radionuclides in the Environment," in press, *ANS Transactions,* **86** (2002).

[6] K. J. Hofstetter and D. M. Beals, "Simplified Model for In-Situ Survey of Gamma Activity in Soil," *Waste Management Symposia 2002* (in press).

[7] K.J. Hofstetter, D.M. Beals and L.S. Nichols, "Estimated ^{137}Cs Inventory in the Fourmile Creek Watershed at SRS," in press, Spectrum 2002 Conference Proceedings, August 2002.

[8] "An Aerial Radiological Survey of the Savannah River Site and Surrounding Area 1998," *EG&G/EM Report* (in press).

[9] K.M. Miller and P. Shebell, "*In-situ* Gamma-Ray Spectrometry – A Tutorial for Environmental Radiation Scientists," US DOE Report EML-557, October 1995.

[10] J.-P. Laedermann, F. Byrde and C. Murith, "*In-situ* Gamma-Ray Spectrometry: the Influence of Topography of the Accuracy of Activity Determination," *J. Environ. Radioactivity*, **38**, No. 1, 1-16, 1998.

[11] L. Curie, *Analytical Chemistry*, **40**, 586, 1968.

Appendix A: Transect 1

location	residual cps (0-2000 keV)	Cs-137 cps (662 keV)	Cs-137 (pCi/g)	2s error
FMB 01-04	38	<0.49	<10.3	
FMB 01-05	37	<0.44	<9.5	
FMB 01-06	45	<0.58	<12.3	
FMB 01-07	55	0.81	17.3	6.2
FMB 01-08	81	4.24	90.2	9.7
FMB 01-09	75	3.21	68.3	8.9
FMB 01-10	122	2.78	59.3	10.6
FMB 01-11	82	0.89	19.0	6.8
FMB 01-12	97	2.89	61.6	9.5
FMB 01-13	83	1.35	28.7	7.6
FMB 01-14	103	2.94	62.5	9.5
FMB 01-15	78	<0.78	<16.5	
FMB 01-16	91	<0.82	<17.3	
FMB 01-17	108	2.02	43.0	9.7
FMB 01-18	53	1.65	35.0	6.5
FMB 01-19	34	1.33	28.3	5.5
FMB 01-20	84	<0.74	<15.7	
FMB 01-21	59	1.83	38.8	7.5
FMB 01-22	156	3.56	75.7	10.9
FMB 01-23	42	1.68	35.8	6.3
FMB 01-24	93	2.77	58.9	9.3
FMB 01-25	109	<0.84	<18.0	
FMB 01-26	102	3.08	65.5	9.6
FMB 01-27	99	2.03	43.2	9.1
FMB 01-28	76	2.39	50.9	8.1
FMB 01-29	58	0.82	17.4	6.0
FMB 01-30	137	2.84	60.4	10.3
FMB 01-31	42	<0.46	<9.7	
FMB 01-32	60	1.54	32.8	5.8
FMB 01-33	35	1.26	26.9	5.6
FMB 01-34	107	<0.89	<18.9	
FMB 01-35	36	1.22	26.0	5.4
FMB 01-36	62	1.18	25.2	6.3
FMB 01-37	88	0.98	20.8	7.6
FMB 01-38	66	1.51	32.1	6.8
FMB 01-39	61	1.57	33.5	7.0
FMB 01-40	64	1.01	21.5	6.6
FMB 01-41	58	<0.54	<11.5	
FMB 01-42	58	<0.60	<12.9	

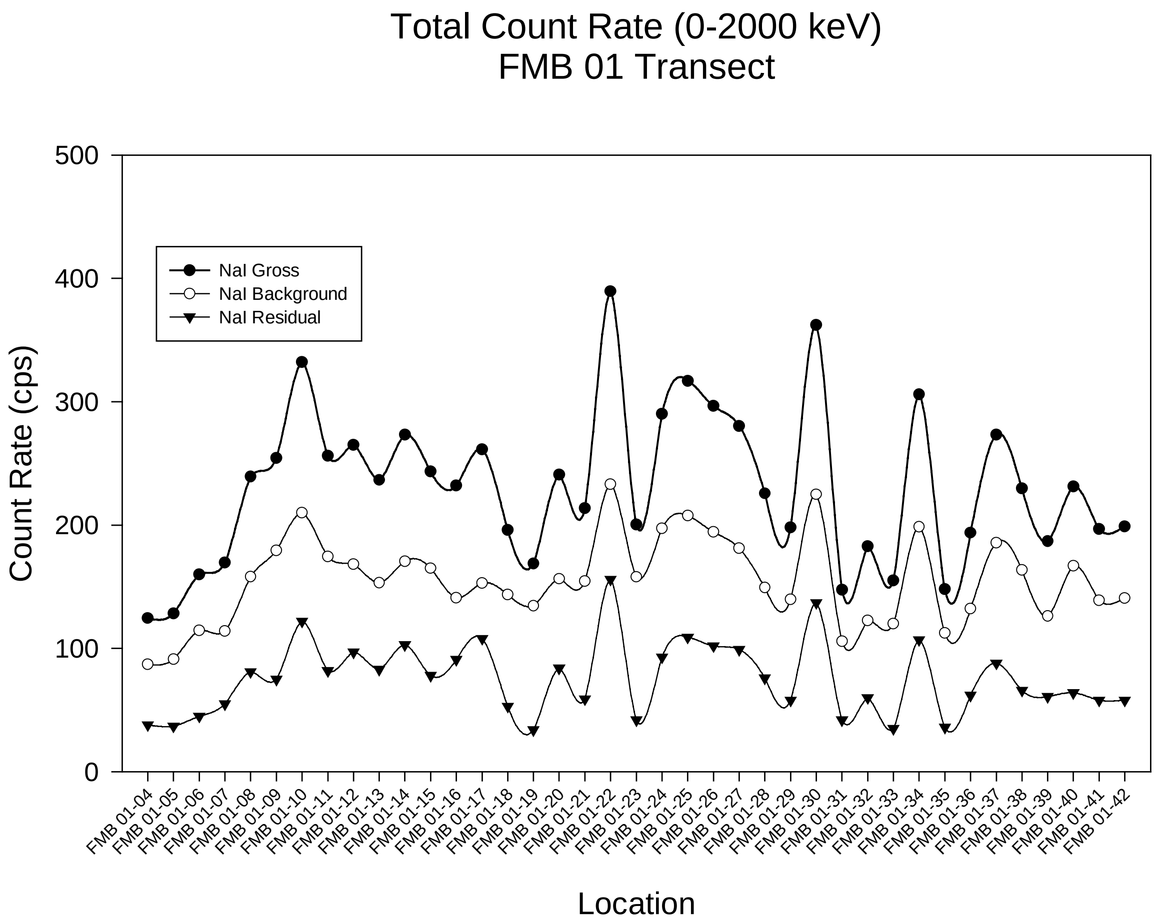

Total Count Rate (0-2000 keV)
FMB 01 Transect
NaI Gross
NaI Background
NaI Residual
Count Rate (cps)
0
100
200
300
400
500
Location
FMB 01-04
FMB 01-05
FMB 01-06
FMB 01-07
FMB 01-08
FMB 01-09
FMB 01-10
FMB 01-11
FMB 01-12
FMB 01-13
FMB 01-14
FMB 01-15
FMB 01-16
FMB 01-17
FMB 01-18
FMB 01-19
FMB 01-20
FMB 01-21
FMB 01-22
FMB 01-23
FMB 01-24
FMB 01-25
FMB 01-26
FMB 01-27
FMB 01-28
FMB 01-29
FMB 01-30
FMB 01-31
FMB 01-32
FMB 01-33
FMB 01-34
FMB 01-35
FMB 01-36
FMB 01-37
FMB 01-38
FMB 01-39
FMB 01-40
FMB 01-41
FMB 01-42

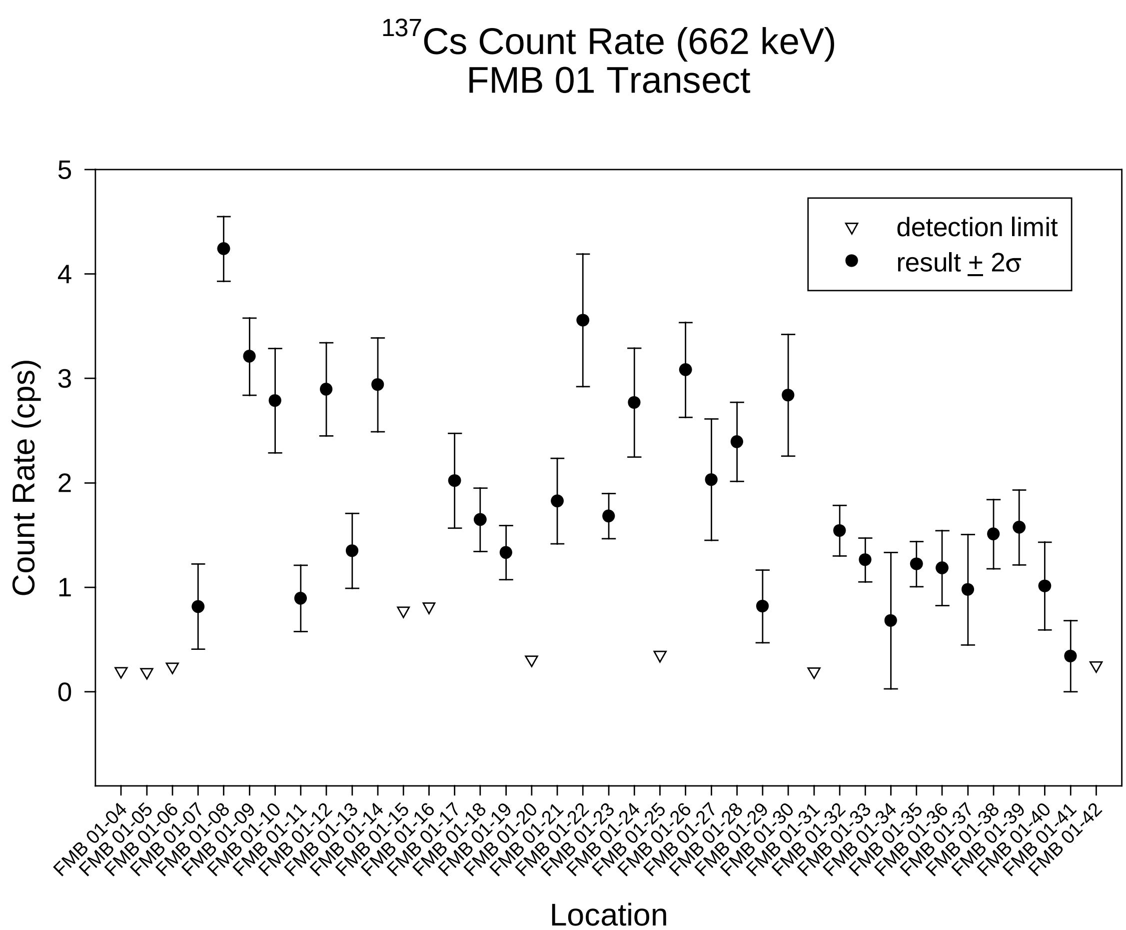

137Cs Count Rate (662 keV)
FMB 01 Transect
detection limit
result ± 2σ
Count Rate (cps)
0
1
2
3
4
5
Location
FMB 01-04
FMB 01-05
FMB 01-06
FMB 01-07
FMB 01-08
FMB 01-09
FMB 01-10
FMB 01-11
FMB 01-12
FMB 01-13
FMB 01-14
FMB 01-15
FMB 01-16
FMB 01-17
FMB 01-18
FMB 01-19
FMB 01-20
FMB 01-21
FMB 01-22
FMB 01-23
FMB 01-24
FMB 01-25
FMB 01-26
FMB 01-27
FMB 01-28
FMB 01-29
FMB 01-30
FMB 01-31
FMB 01-32
FMB 01-33
FMB 01-34
FMB 01-35
FMB 01-36
FMB 01-37
FMB 01-38
FMB 01-39
FMB 01-40
FMB 01-41
FMB 01-42

Core Bore FMB 01-02
near Flag FMB 01-24

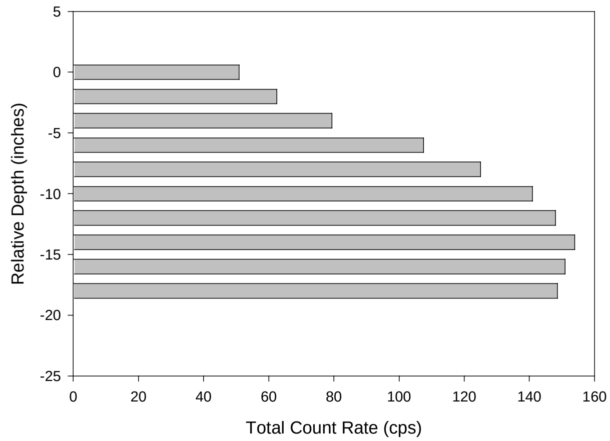

Count Rate Core Bore FMB 01-02
^{137}Cs (662 keV) Photopeak
8/17/01

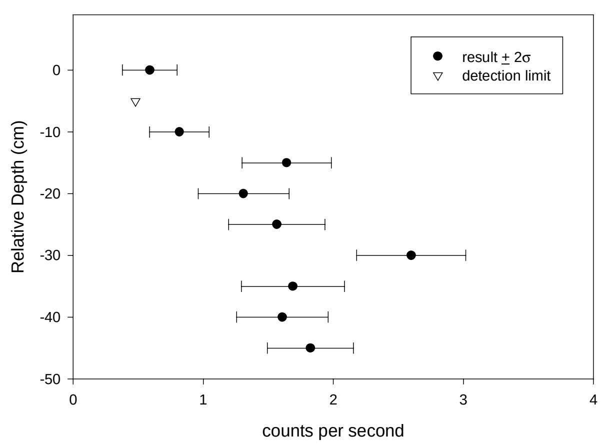

distance to detector cm	soil absorber cm	SYNTH count rate cps	observed count rate cps	fraction	product
30	0	0.2392	0.6	0.058	0.014
35	5	0.1507	<0.5		
40	10	0.0904	0.8	0.080	0.007
45	15	0.0564	1.6	0.161	0.009
50	20	0.04295	1.3	0.128	0.006
55	25	0.02825	1.6	0.153	0.004
60	30	0.01725	2.6	0.254	0.004
65	35	0.01385	1.7	0.165	0.002

total= 10.2 sum= 0.047

Appendix B: Tansect 2

location	residual cps (0-2000 keV)	Cs-137 cps (662 keV)	Cs-137 (pCi/g)	2s error
FMB 02-04	53	<0.73	<12.8	
FMB 02-05	52	<0.64	<11.3	
FMB 02-06	55	0.70	12.2	5.6
FMB 02-07	54	<0.61	<10.7	
FMB 02-08	57	<0.70	<12.3	
FMB 02-09	70	1.94	34.0	7.1
FMB 02-10	79	2.83	49.7	7.7
FMB 02-11	95	<0.91	<15.9	
FMB 02-12	67	2.00	35.1	6.1
FMB 02-13	58	<0.65	<11.4	
FMB 02-14	53	2.80	49.1	6.7
FMB 02-15	63	<0.76	<13.4	
FMB 02-16	71	1.68	29.5	6.8
FMB 02-17	152	3.76	65.9	10.0
FMB 02-18	61	<0.74	<13.0	
FMB 02-19	60	0.97	17.0	6.4
FMB 02-20	47	<0.48	<8.5	
FMB 02-21	62	2.30	40.3	6.6
FMB 02-22	125	3.64	63.8	9.1
FMB 02-23	55	<0.64	<11.3	
FMB 02-24	57	<0.62	<11.0	
FMB 02-25	61	1.44	25.3	5.6
FMB 02-26	63	<0.74	<12.9	
FMB 02-27	64	0.93	16.4	5.5
FMB 02-28	179	4.33	75.9	11.4
FMB 02-29	112	4.56	79.9	9.7
FMB 02-30	79	2.62	45.9	7.5
FMB 02-31	86	3.03	53.1	7.9
FMB 02-32	131	5.27	92.5	9.8
FMB 02-33	140	5.46	95.8	9.9
FMB 02-34	128	5.34	93.7	10.1
FMB 02-34	142	4.57	80.2	9.7
FMB 02-35	191	6.77	118.9	10.8
FMB 02-36	93	1.68	29.4	7.4
FMB 02-37	150	9.69	169.9	12.5
FMB 02-38	83	1.53	26.9	6.6
FMB 02-39	119	4.89	85.8	9.2
FMB 02-40	80	<0.69	<12.1	
FMB 02-41	81	<0.62	<10.9	
FMB 02-42	76	<0.73	<12.9	
FMB 02-43	73	<0.73	<12.8	
FMB 02-44	62	1.50	26.4	5.9
FMB 02-45	52	<0.59	<10.3	
FMB 02-46	77	2.56	44.9	7.0
FMB 02-47	67	<0.71	<12.4	
FMB 02-48	65	<0.63	<11.1	
FMB 02-49	58	0.93	16.3	5.4
FMB 02-50	62	<0.67	<11.8	

Total Count Rate (0-2000 keV)
FMB 02 Transect

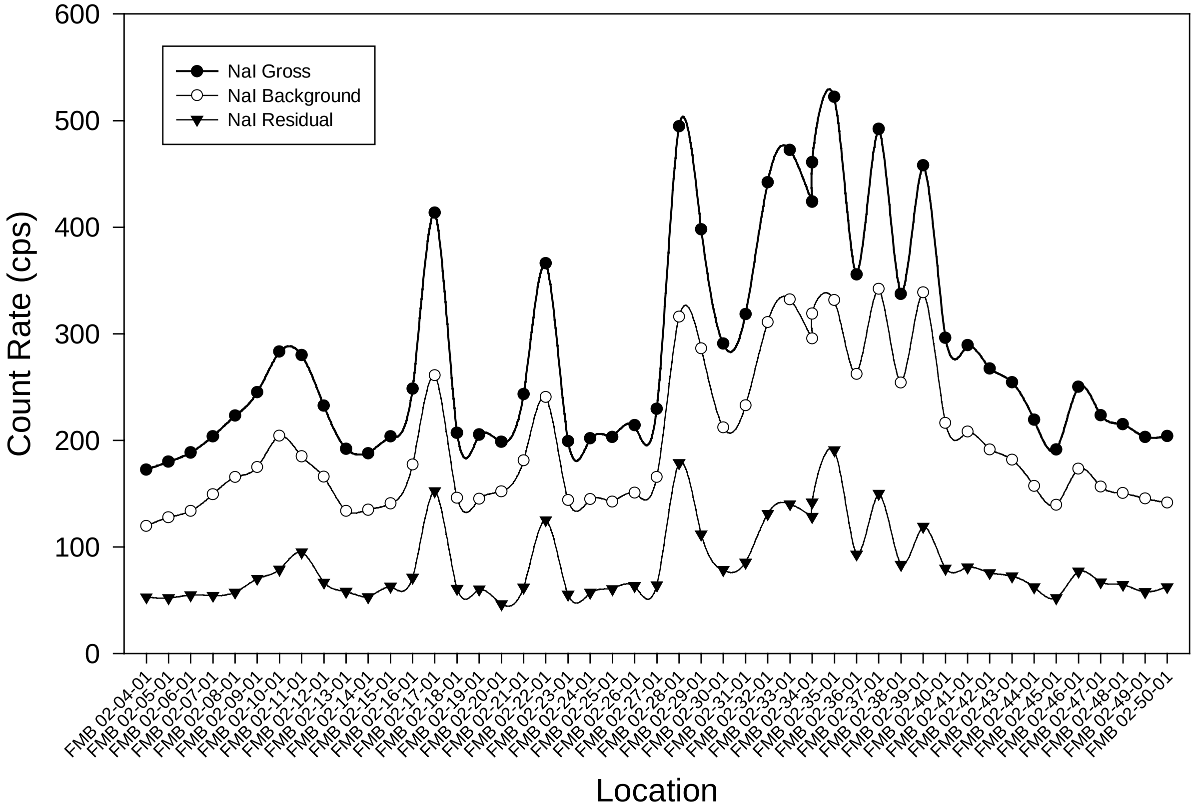

^{137}Cs Count Rate (662 keV)
FMB 02 Transect

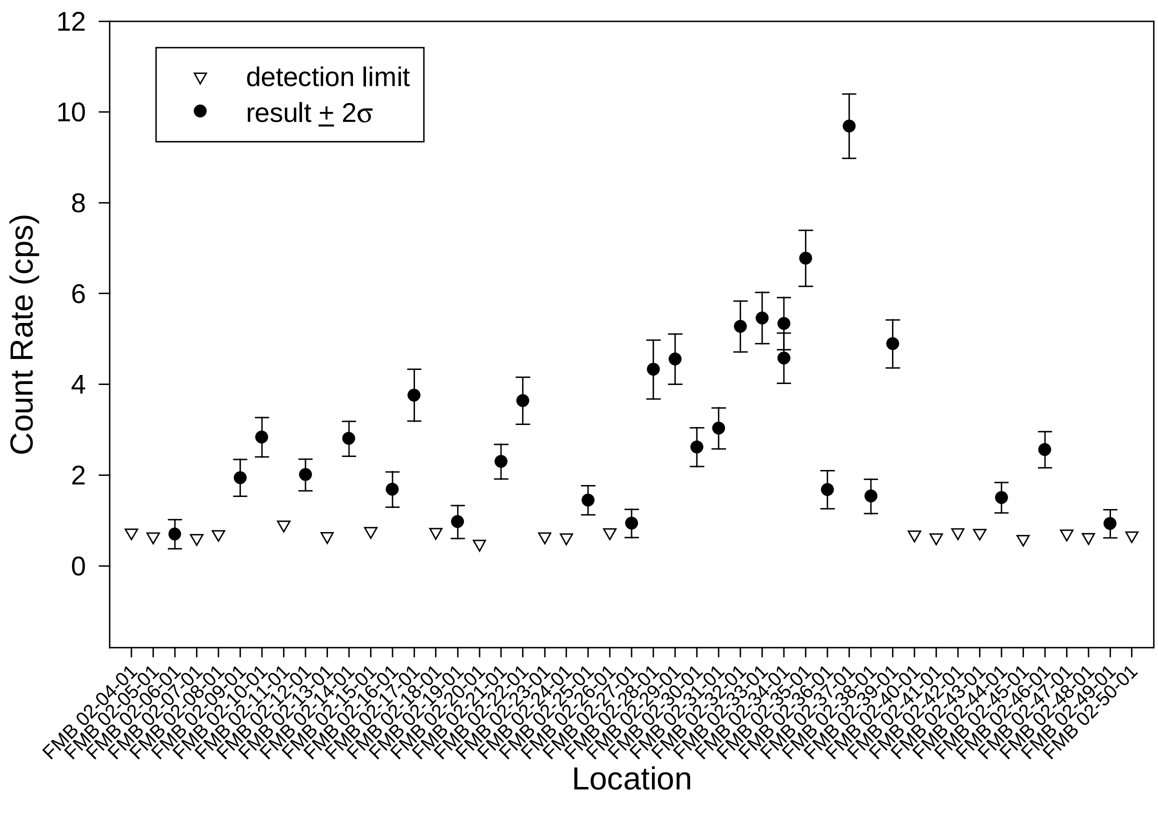

Bore Hole FMB 02-02
Near Flag FMB 02-28

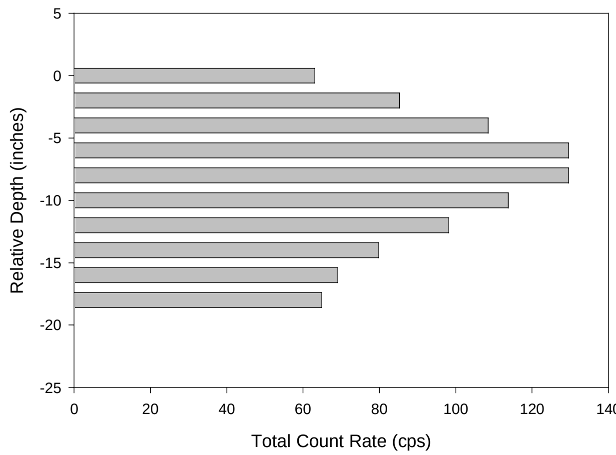

Count Rate Core Bore FMB 02-02
^{137}Cs (662 keV) ROI
7/27/01

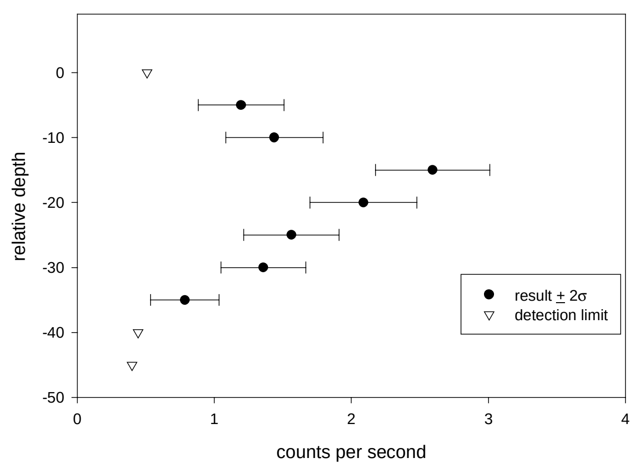

distance to detector cm	soil absorber cm	SYNTH count rate cps	observed count rate cps	fraction	product
30	0	0.2392	<0.5		
35	5	0.1507	1.2	0.108	0.016
40	10	0.0904	1.4	0.130	0.012
45	15	0.0564	2.6	0.235	0.013
50	20	0.04295	2.1	0.189	0.008
55	25	0.02825	1.6	0.142	0.004
60	30	0.01725	1.4	0.123	0.002
65	35	0.01385	0.8	0.071	0.001

total= 11.0 sum= 0.057

Appendix C: Transect 3

location	residual cps (0-2000 keV)	Cs-137 cps (662 keV)	Cs-137 (pCi/g)	2s error
FMB 03-04	55	<0.55	<6.5	
FMB 03-05	55	<0.62	<7.2	
FMB 03-06	62	<0.67	<7.8	
FMB 03-07	69	<0.80	<9.3	
FMB 03-08	68	<0.72	<8.4	
FMB 03-09	64	<0.59	<6.9	
FMB 03-10	65	<0.45	<5.2	
FMB 03-11	66	<0.52	<6.1	
FMB 03-12	59	<0.57	<6.6	
FMB 03-13	64	1.07	12.4	2.8
FMB 03-14	65	<0.49	<5.7	
FMB 03-15	81	1.87	21.8	4.0
FMB 03-16	87	0.54	6.3	2.1
FMB 03-17	71	<0.62	<7.2	
FMB 03-18	87	3.06	35.5	4.6
FMB 03-19	85	2.30	26.7	4.6
FMB 03-20	48	0.62	7.2	2.4
FMB 03-21	61	<0.41	<4.7	
FMB 03-22	66	<0.54	<6.3	
FMB 03-23	69	<0.56	<6.4	
FMB 03-24	56	<0.56	<6.5	
FMB 03-25	71	<0.71	<8.3	
FMB 03-26	64	1.61	18.7	4.1
FMB 03-27	83	<0.70	<8.1	
FMB 03-28	66	0.84	9.8	3.7
FMB 03-29	58	<0.64	<7.4	
FMB 03-30	56	<0.66	<7.6	
FMB 03-31	56	1.45	16.8	3.5
FMB 03-32	52	<0.60	<7.0	
FMB 03-33	53	<0.64	<7.4	
FMB 03-34	55	<0.54	<6.3	
FMB 03-35	53	0.70	8.2	3.5
FMB 03-36	99	3.20	37.2	5.4
FMB 03-37	74	2.29	26.6	3.7
FMB 03-38	71	0.92	10.8	3.8
FMB 03-39	74	1.84	21.4	4.1
FMB 03-40	78	3.14	36.5	4.6
FMB 03-41	94	1.42	16.5	4.6
FMB 03-42	103	2.33	27.1	5.0
FMB 03-43	59	2.83	32.9	4.4
FMB 03-44	99	4.24	49.3	5.8
FMB 03-45	97	1.96	22.8	4.5
FMB 03-46	59	<0.65	<7.5	
FMB 03-47	56	<0.65	<7.6	
FMB 03-48	56	<0.64	<7.5	
FMB 03-49	55	1.48	17.3	3.9
FMB 03-50	51	2.18	25.3	3.8
FMB 03-51	51	<0.63	<7.3	
FMB 03-52	54	1.21	14.0	3.4
FMB 03-53	43	<0.49	<5.7	
FMB 03-54	45	<0.60	<7.0	
FMB 03-55	45	<0.55	<6.4	
FMB 03-56	52	<0.56	<6.5	
FMB 03-57	50	0.93	10.8	3.7
FMB 03-58	46	<0.59	<6.9	

Total Count Rate (0-2000 keV)
FMB 03 Transect

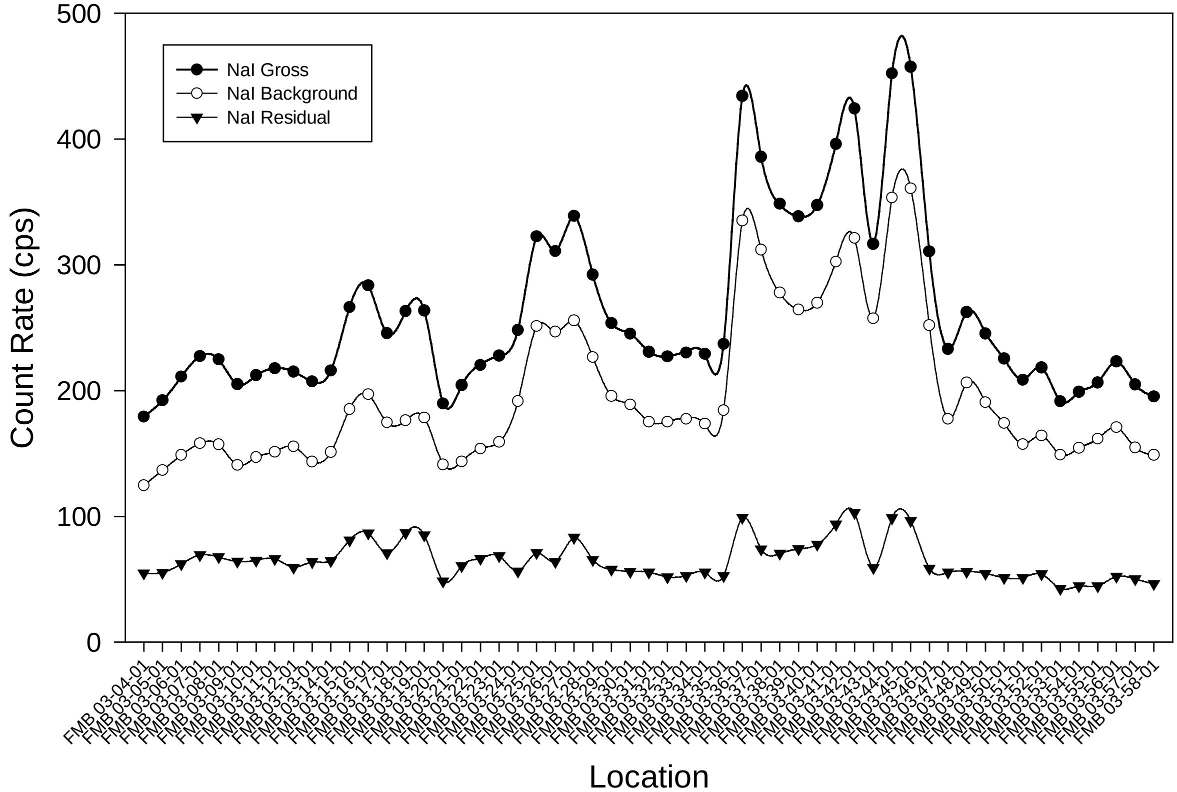

^{137}Cs Count Rate (662 keV)
FMB 03 Transect

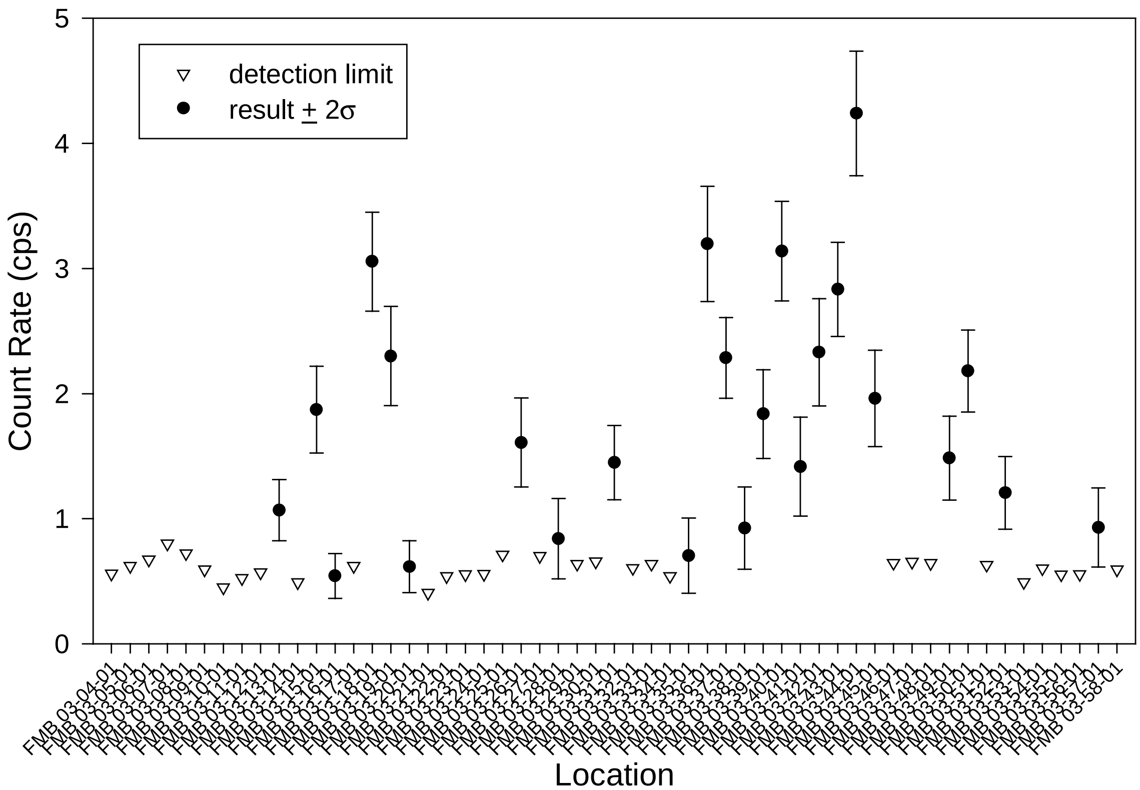

Bore Hole FMB 03-02
W of Flag FMB 03-36

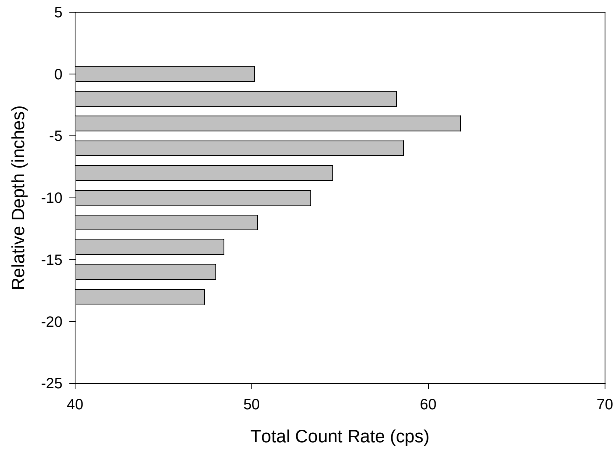

Core Bore FMB 03-02
7/26/01
Cs-137 (662 keV)

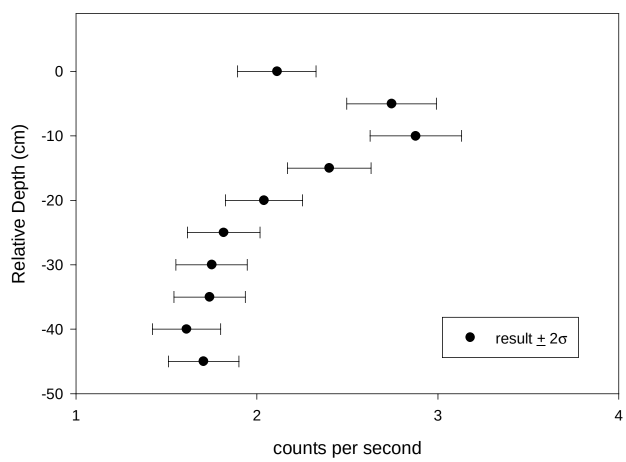

distance to detector cm	soil absorber cm	SYNTH count rate cps	observed count rate cps	fraction	product
30	0	0.2392	2.1	0.121	0.029
35	5	0.1507	2.7	0.157	0.024
40	10	0.0904	2.9	0.165	0.015
45	15	0.0564	2.4	0.137	0.008
50	20	0.04295	2.0	0.117	0.005
55	25	0.02825	1.8	0.104	0.003
60	30	0.01725	1.8	0.100	0.002
65	35	0.01385	1.7	0.099	0.001

total= 17.5 sum= 0.086

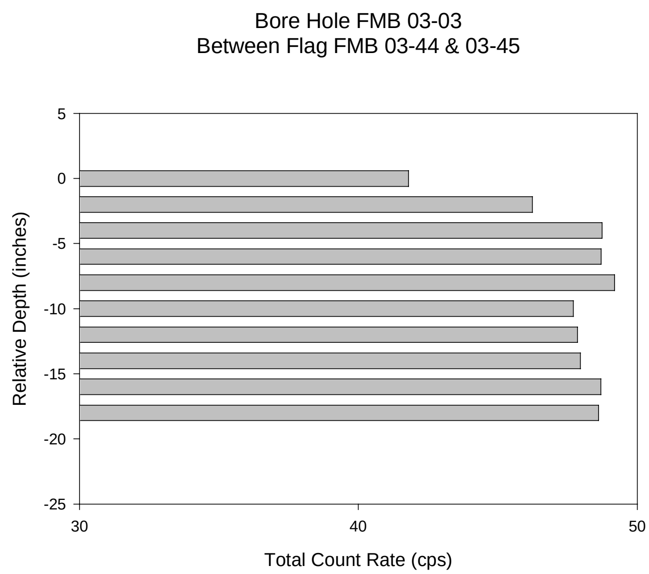
Bore Hole FMB 03-03
Between Flag FMB 03-44 & 03-45
5
0
-5
-10
-15
-20
-25
30
40
50
Relative Depth (inches)
Total Count Rate (cps)

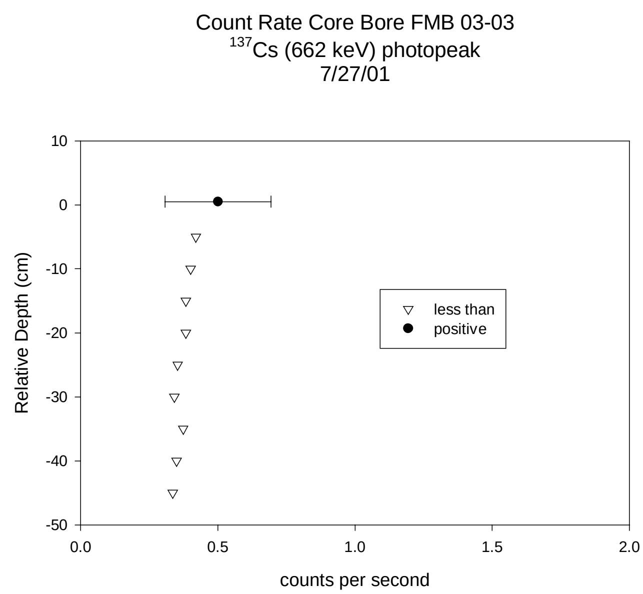
Count Rate Core Bore FMB 03-03
137Cs (662 keV) photopeak
7/27/01
10
0
-10
-20
-30
-40
-50
0.0
0.5
1.0
1.5
2.0
Relative Depth (cm)
counts per second
less than
positive

Appendix D: Transect 4

location	residual cps	Cs-137 cps	Cs-137	
	(0-2000 keV)	(662 keV)	(pCi/g)	2s error
FMB 04-01	71	<0.60	<7.5	
FMB 04-02	413	19.67	245.8	10.9
FMB 04-03	82	5.01	62.7	5.2
FMB 04-04	100	4.23	52.9	5.4
FMB 04-05	46	1.46	18.3	3.5
FMB 04-06	137	8.85	110.6	6.1
FMB 04-07	67	0.81	10.2	3.1
FMB 04-08	43	<0.45	<5.6	
FMB 04-09	27	<0.47	<5.9	
FMB 04-10	78	1.36	17.0	4.5

FMB-A4 Transect
10/31/01 & 12/03/01

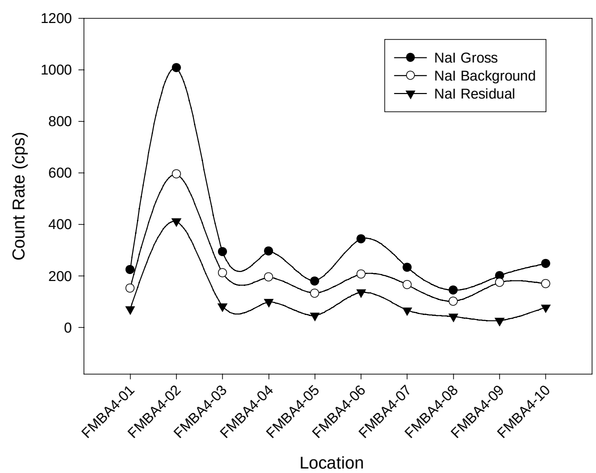

FMBA4 Transect
^{137}Cs (662 keV)

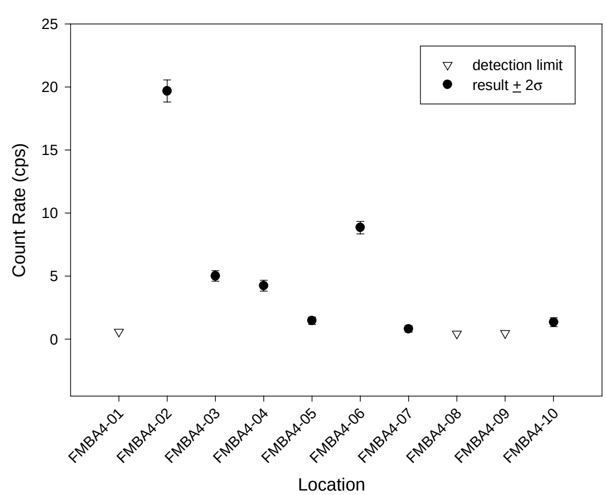

Appendix E: Transect 5

location	residual cps (0-2000 keV)	Cs-137 cps (662 keV)	Cs-137 (pCi/g)	2s error
FMB 05-01	30	<0.41	<5.1	
FMB 05-02	55	<0.52	<6.5	
FMB 05-03	54	1.40	17.5	4.0
FMB 05-04	49	0.57	7.1	4.4
FMB 05-05	49	0.90	11.2	4.2
FMB 05-06	85	4.36	54.5	4.9
FMB 05-07	135	6.33	79.2	8.4
FMB 05-08	46	<0.54	<6.8	
FMB 05-09	49	<0.41	<5.1	

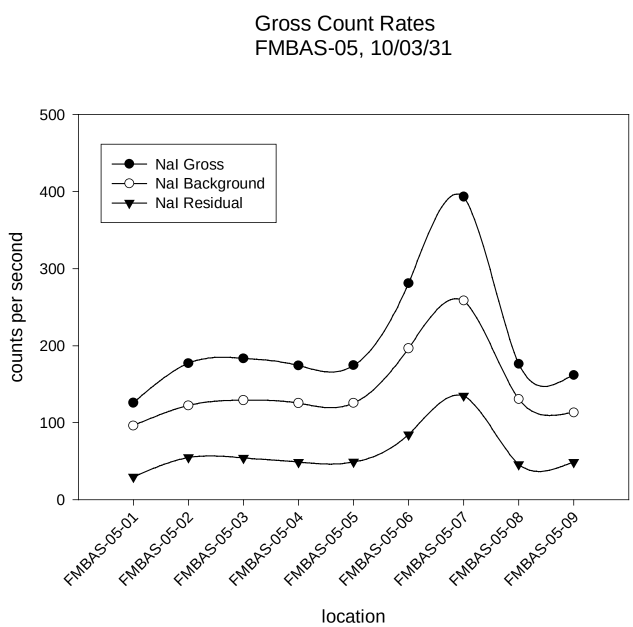

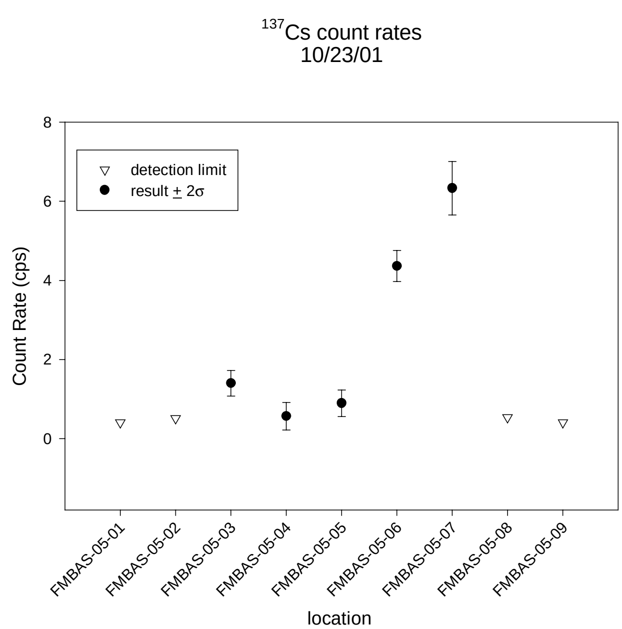

Appendix F: Transect 6

location	residual cps (0-2000 keV)	Cs-137 cps (662 keV)	Cs-137 (pCi/g)	2s error
FMB 06-01	51	<0.54	<6.8	
FMB 06-02	54	<0.47	<5.9	
FMB 06-03	52	<0.41	<5.1	
FMB 06-04	44	<0.39	<4.9	
FMB 06-05	74	1.65	20.6	3.3
FMB 06-06	45	<0.43	<5.4	

Gross Count Rates
FMBAS-06, 10/03/01

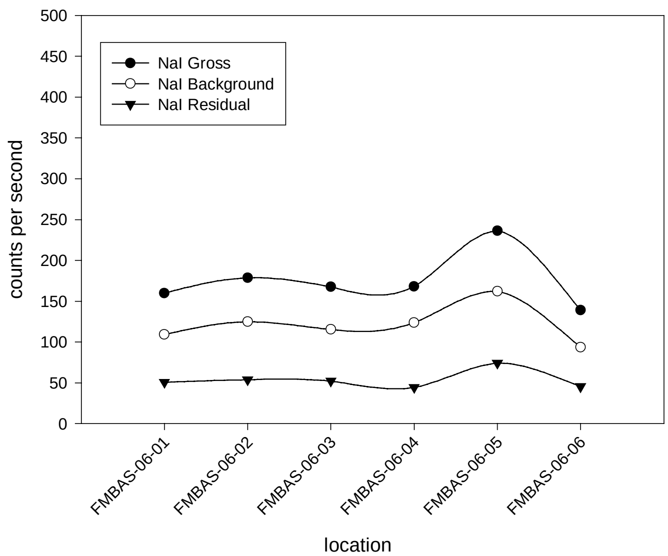

^{137}Cs count rates
10/18/01

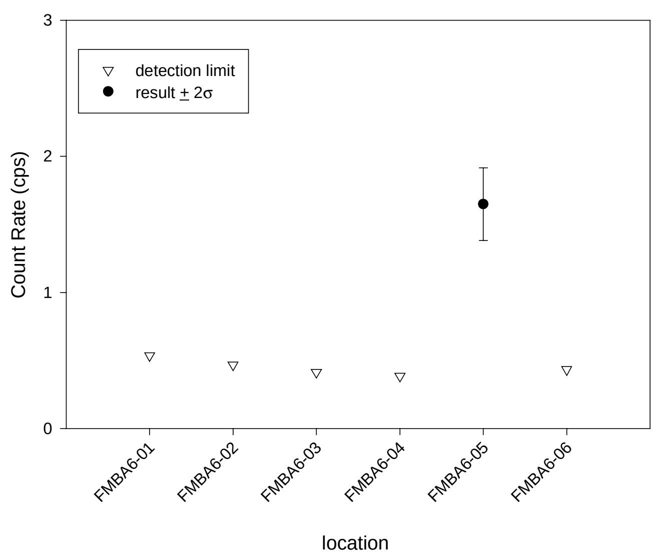

Appendix G: Transect 7

location	residual cps (0-2000 keV)	Cs-137 cps (662 keV)	Cs-137 (pCi/g)	2s error
FMB 07-01	231	14.33	183.7	8.9
FMB 07-02	548	37.75	483.9	15.5
FMB 07-03	193	7.13	91.5	9.0
FMB 07-04	275	13.43	172.1	10.3
FMB 07-05	272	15.90	203.9	9.8
FMB 07-06	128	4.33	55.5	6.0
FMB 07-07	618	31.72	406.6	15.5
FMB 07-08	161	2.84	36.4	8.0
FMB 07-09	205	9.20	118.0	7.5
FMB 07-10	774	28.10	360.3	17.8
FMB 07-11	163	5.91	75.8	8.5
FMB 07-12	444	19.13	245.2	12.8
FMB 07-13	898	35.75	458.3	17.1
FMB 07-14	463	26.08	334.3	13.6
FMB 07-15	334	15.39	197.3	10.9
FMB 07-16	64	1.53	19.6	5.3
FMB 07-17	159	9.55	122.4	6.7
FMB 07-18	562	24.32	311.8	13.9
FMB 07-19	361	20.03	256.8	10.8
FMB 07-20	409	18.92	242.6	12.2
FMB 07-21	532	10.30	132.1	14.9
FMB 07-22	331	6.23	79.9	8.0
FMB 07-23	140	6.10	78.2	7.5

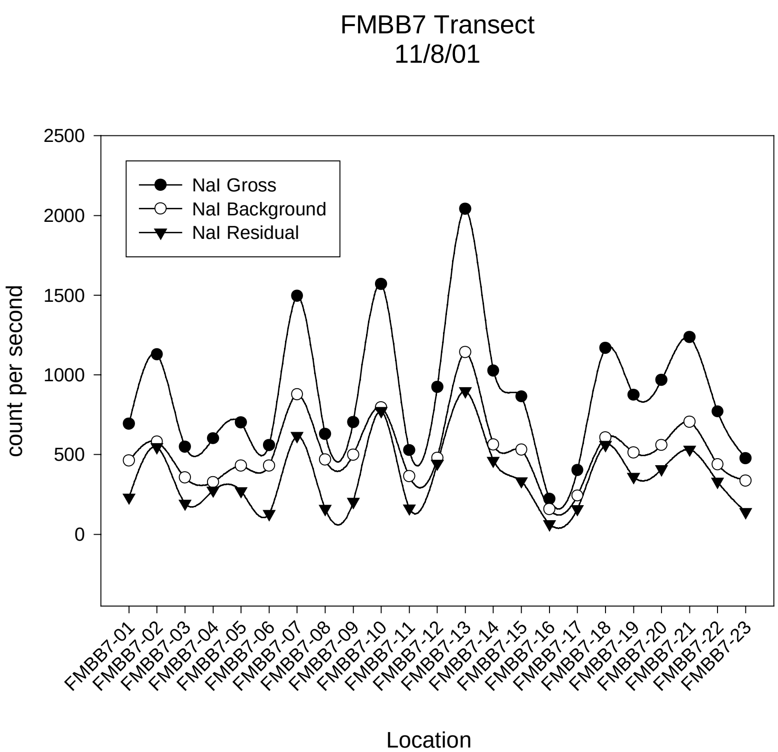

FMBB7 Transect
^{137}Cs (662 keV)
11/8/01

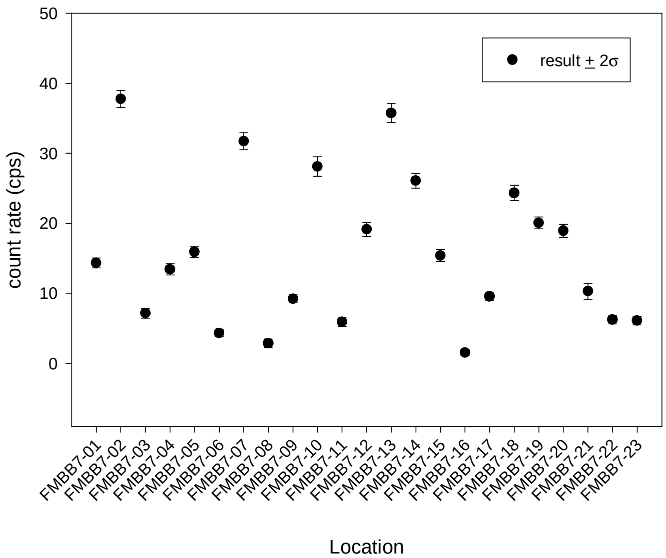

Bore Hole FMBB7-24
^{137}Cs (662 keV) Count Rate
12/6/02

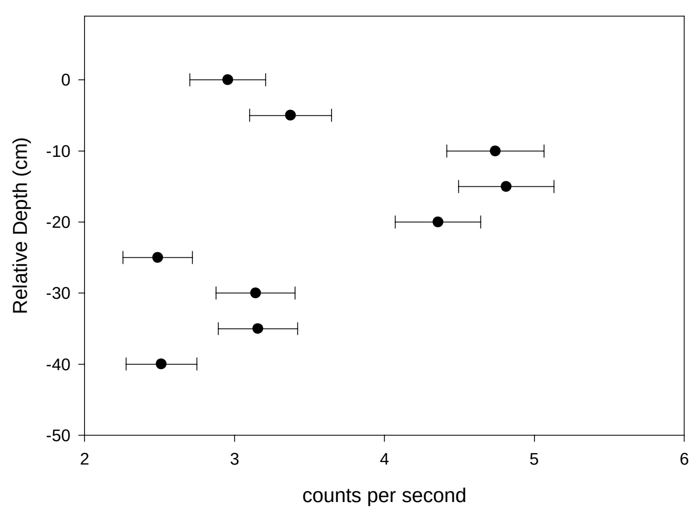

distance to detector cm	soil absorber cm	SYNTH count rate cps	observed count rate cps	fraction	product
30	0	0.2392	3.0	0.102	0.024
35	5	0.1507	3.4	0.116	0.017
40	10	0.0904	4.7	0.163	0.015
45	15	0.0564	4.8	0.166	0.009
50	20	0.04295	4.4	0.150	0.006
55	25	0.02825	2.5	0.086	0.002
60	30	0.01725	3.1	0.108	0.002
65	35	0.01385	3.2	0.109	0.002

total= 29.0 sum= 0.078

Appendix H: Transect 8

location	residual cps (0-2000 keV)	Cs-137 cps (662 keV)	Cs-137 (pCi/g)	2s error
FMB 08-01	30	0.62	8.2	
FMB 08-02	44	<0.40	<5.4	
FMB 08-03	48	<0.34	<4.5	
FMB 08-04	90	<0.57	<7.6	
FMB 08-05	138	6.30	84.0	6.4
FMB 08-06	101	3.93	52.3	3.6
FMB 08-07	98	0.82	11.0	4.6
FMB 08-08	83	0.70	9.4	2.9
FMB 08-09	81	<0.48	<6.4	
FMB 08-10	112	<0.56	<7.4	

Gross Count Rates
FMBAS-08, 10/03/01

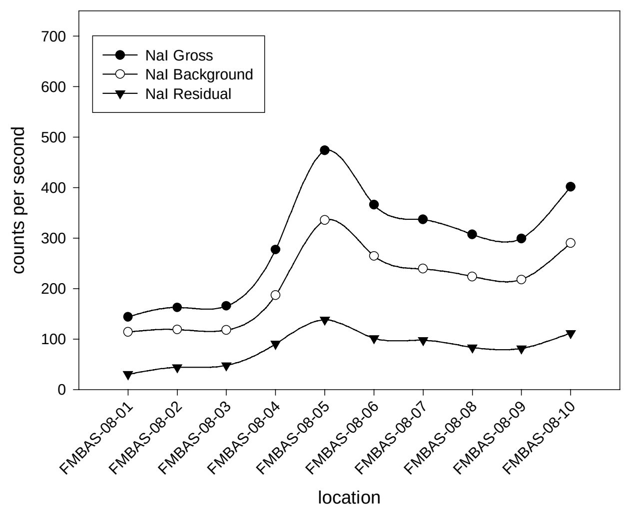

^{137}Cs count rates
10/23/01

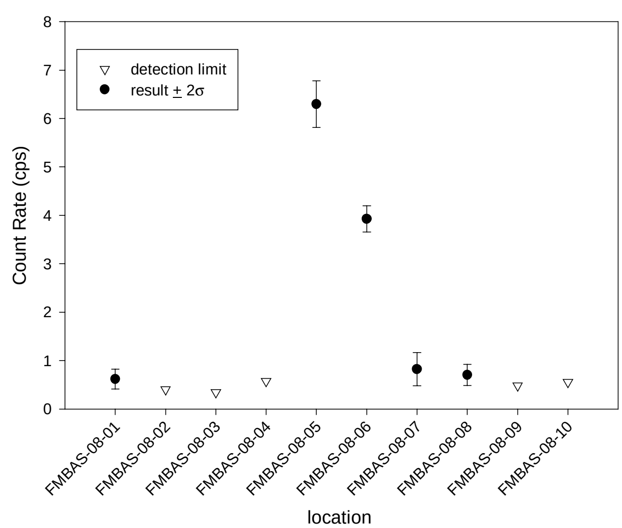

Appendix I: Transect 9

location	residual cps (0-2000 keV)	Cs-137 cps (662 keV)	Cs-137 (pCi/g)	2s error
FMB 09-01	36	0.73	9.7	3.2
FMB 09-02	33	0.53	7.1	3.7
FMB 09-03	32	0.46	6.1	2.0
FMB 09-04	62	<0.49	<6.6	
FMB 09-05	772	27.82	371.0	16.4
FMB 09-06	381	21.83	291.1	11.6
FMB 09-07	772	38.23	509.7	19.1
FMB 09-08	73	<0.44	<5.9	
FMB 09-09	59	0.59	7.8	2.2
FMB 09-10	57	0.55	7.4	0.7

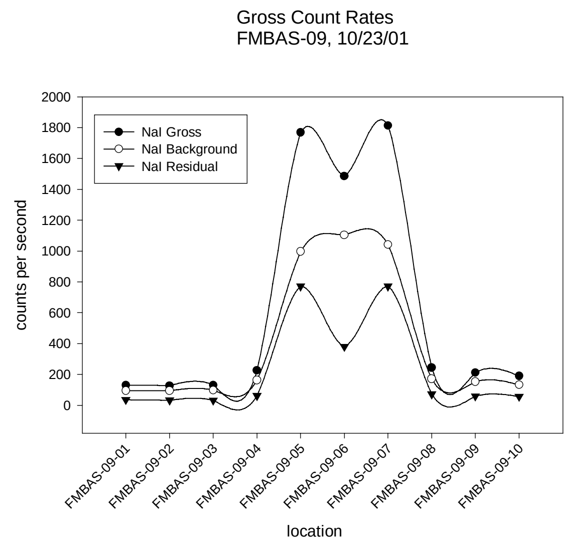

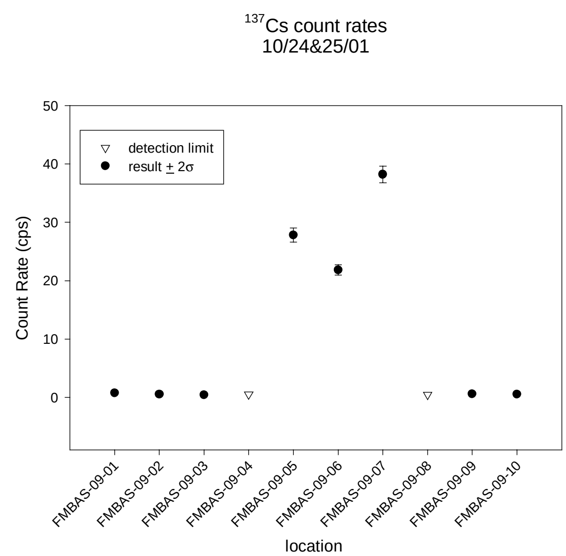

Appendix J: Transect 10

location	residual cps (0-2000 keV)	Cs-137 cps (662 keV)	Cs-137 (pCi/g)	2s error
FMB 10-01	45	<0.44	<5.9	
FMB 10-02	56	1.16	15.5	4.7
FMB 10-03	38	1.06	14.1	2.5
FMB 10-04	47	<0.39	<5.2	
FMB 10-05	523	22.85	304.7	15.5
FMB 10-06	688	26.29	350.5	18.1
FMB 10-07	412	8.96	119.5	10.0
FMB 10-08	40	0.37	4.9	5.9
FMB 10-09	28	0.19	2.6	2.2
FMB 10-10	22	<0.28	<3.7	

Gross Count Rates
FMBAS-10, 10/24&25/01

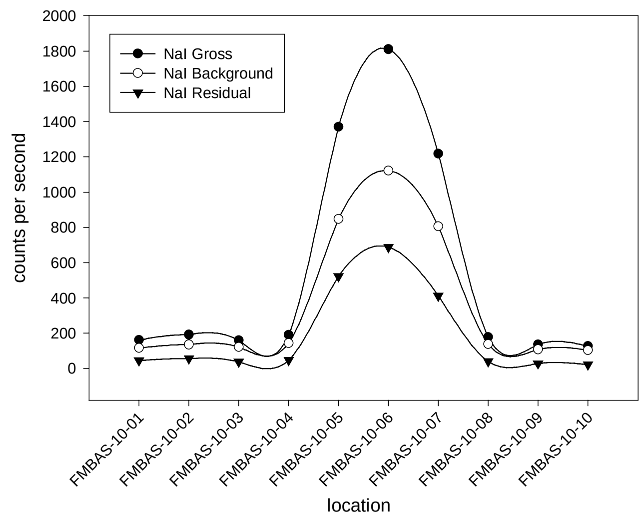

^{137}Cs count rates
10/24&25/01

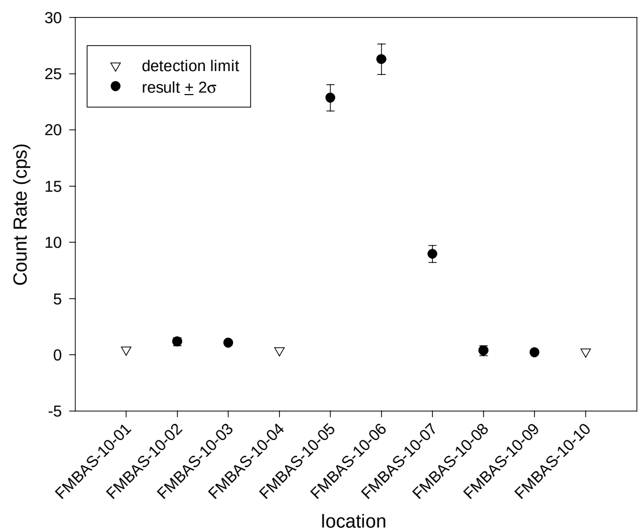

Appendix K: Transect 11

location	residual cps (0-2000 keV)	Cs-137 cps (662 keV)	Cs-137 (pCi/g)	2s error
FMB 11-01	411	21.01	291.9	11.3
FMB 11-02	402	16.89	234.5	10.2
FMB 11-03	284	11.84	164.4	8.0
FMB 11-04	570	26.17	363.5	13.7
FMB 11-05	401	14.93	207.3	11.7
FMB 11-06	695	27.76	385.6	15.0
FMB 11-07	563	24.62	341.9	12.7
FMB 11-08	483	18.48	256.7	11.5
FMB 11-09	293	13.08	181.7	10.3
FMB 11-10	71	4.50	62.5	3.6

FMBC-11 Transect
11/6/01

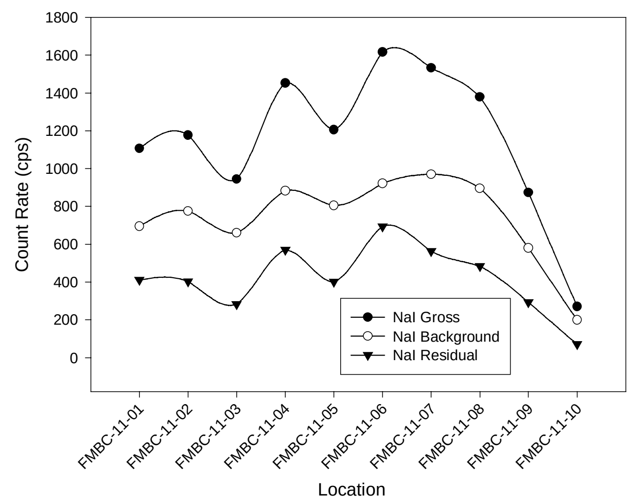

FMBC-11 Transect
^{137}Cs Rate (662 keV)
11/6/01

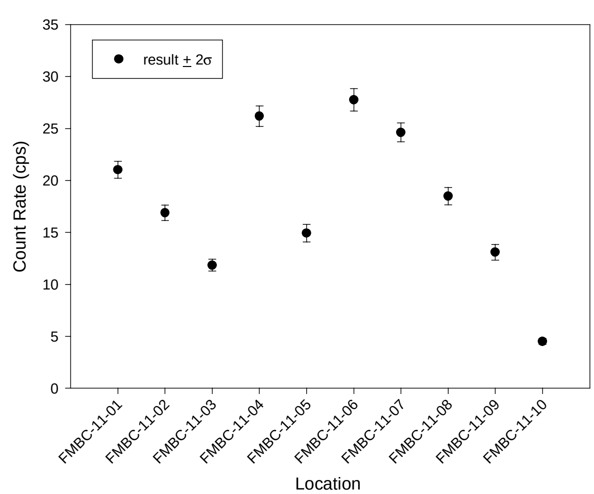

Bore Hole FMBC11-11
^{137}Cs (662 keV) Count Rate
12/6/01

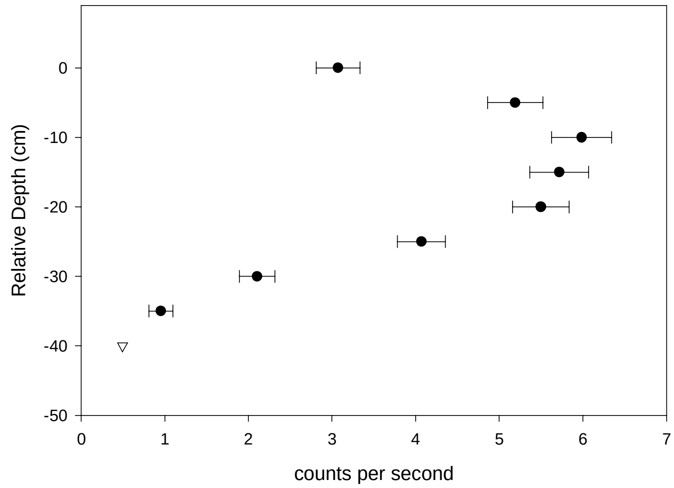

distance to detector cm	soil absorber cm	SYNTH count rate cps	observed count rate cps	fraction	product
30	0	0.2392	3.1	0.094	0.023
35	5	0.1507	5.2	0.159	0.024
40	10	0.0904	6.0	0.184	0.017
45	15	0.0564	5.7	0.175	0.010
50	20	0.04295	5.5	0.169	0.007
55	25	0.02825	4.1	0.125	0.004
60	30	0.01725	2.1	0.065	0.001
65	35	0.01385	1.0	0.029	0.000

total= 32.6 sum= 0.085

Bore Hole FMBC11-13
^{137}Cs (662 keV) Count Rates
12/6/01

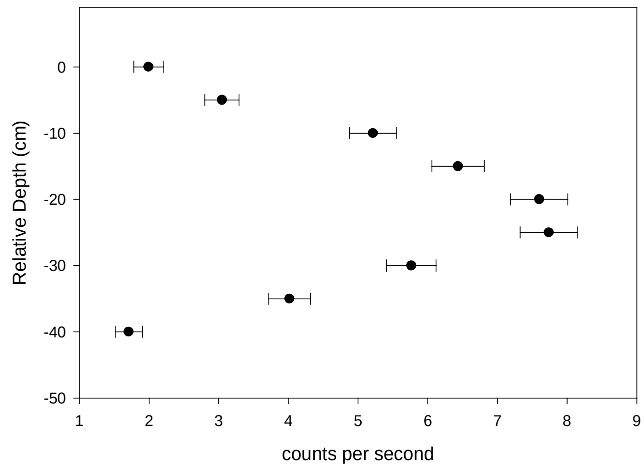

distance to detector cm	soil absorber cm	SYNTH count rate cps	observed count rate cps	fraction	product
30	0	0.2392	2.0	0.048	0.011
35	5	0.1507	3.0	0.073	0.011
40	10	0.0904	5.2	0.125	0.011
45	15	0.0564	6.4	0.154	0.009
50	20	0.04295	7.6	0.182	0.008
55	25	0.02825	7.7	0.185	0.005
60	30	0.01725	5.8	0.138	0.002
65	35	0.01385	4.0	0.096	0.001

total= 41.8 sum= 0.059

Appendix L: Transect 12

location	residual cps	Cs-137 cps	Cs-137	
	(0-2000 keV)	(662 keV)	(pCi/g)	2s error
FMB 12-01	32	<0.30	<4.2	
FMB 12-02	21	<0.25	<3.4	
FMB 12-03	21	0.46	6.4	0.5
FMB 12-04	52	0.48	6.6	3.1
FMB 12-05	86	2.36	32.8	4.8
FMB 12-06	534	18.47	256.6	12.7
FMB 12-07	1067	40.03	555.9	20.4
FMB 12-08	77	0.89	12.3	4.1
FMB 12-09	53	0.81	11.3	2.9
FMB 12-10	46	<0.33	<4.5	
FMB 12-11	47	<0.32	<4.5	

FMBC12 Transect
11/7/01

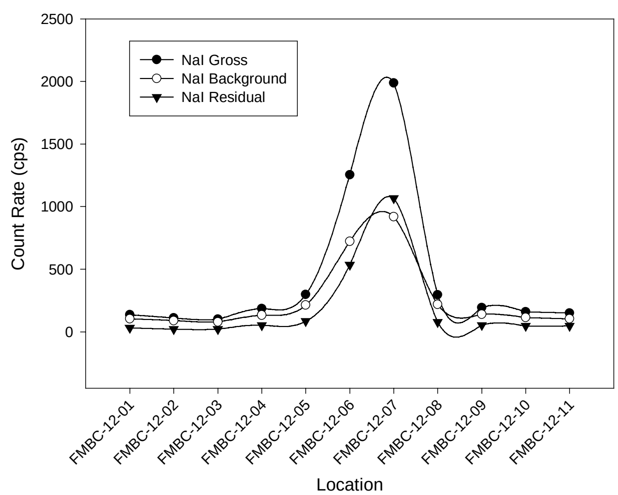

FMBC12 Transect
^{137}Cs (662 keV)
11/7/01

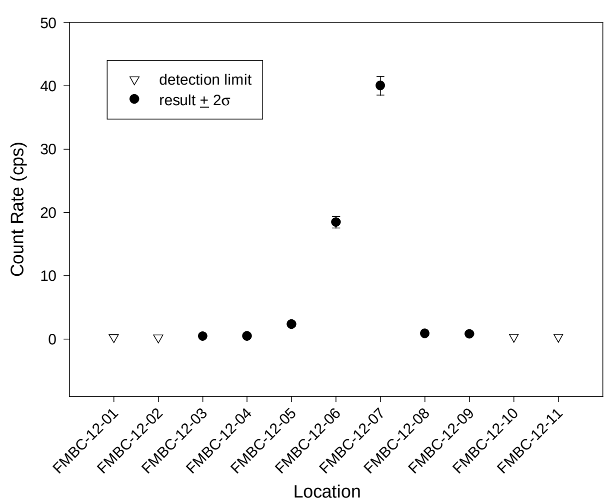

Appendix M: Transect 13

location	residual cps (0-2000 keV)	Cs-137 cps (662 keV)	Cs-137 (pCi/g)	2s error
FMB 13-01	87	3.25	54.2	7.9
FMB 13-02	147	8.43	140.4	10.0
FMB 13-03	106	5.49	91.5	6.7
FMB 13-04	127	6.18	103.0	9.0
FMB 13-05	166	6.15	102.5	10.9
FMB 13-06	285	12.20	203.4	14.3
FMB 13-07	160	6.27	104.5	8.3
FMB 13-08	100	3.14	52.3	9.2
FMB 13-09	40	0.83	13.8	5.7
FMB 13-10	80	3.86	64.4	6.7
FMB 13-11	91	2.52	42.0	8.1

Gross Count Rates
FMBD-13, 11/15/01

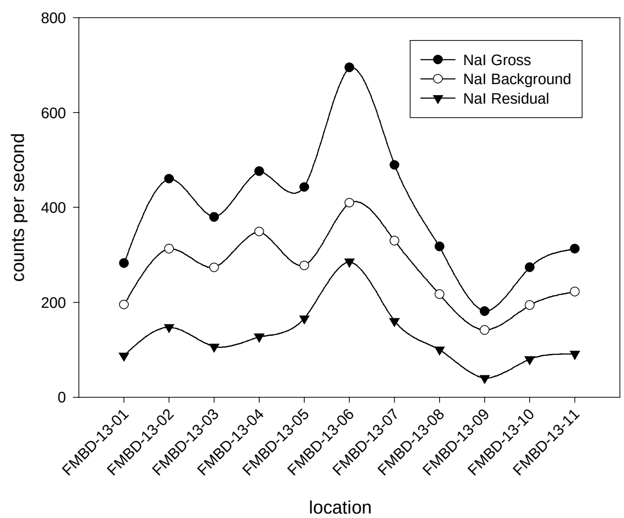

137Cs Count Rate
FMBD-13

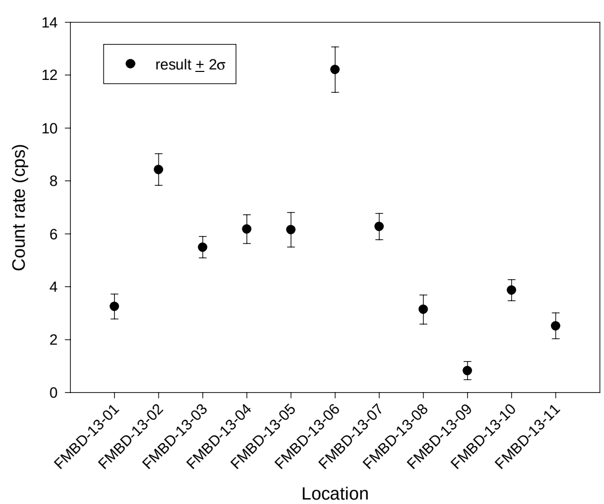

Appendix N: Transect 14

location	residual cps	Cs-137 cps	Cs-137	
	(0-2000 keV)	(662 keV)	(pCi/g)	2s error
FMB 14-01	75	3.94	65.7	5.3
FMB 14-02	265	7.51	125.2	14.5
FMB 14-03	301	12.49	208.2	13.3
FMB 14-04	43	<0.50	<8.3	
FMB 14-05	30	0.98	16.3	2.7
FMB 14-06	17	0.68	11.4	1.0
FMB 14-07	13	<0.24	<3.9	
FMB 14-08	12	<0.20	<3.3	

Gross Count Rates
FMBD-14, 11/13/01

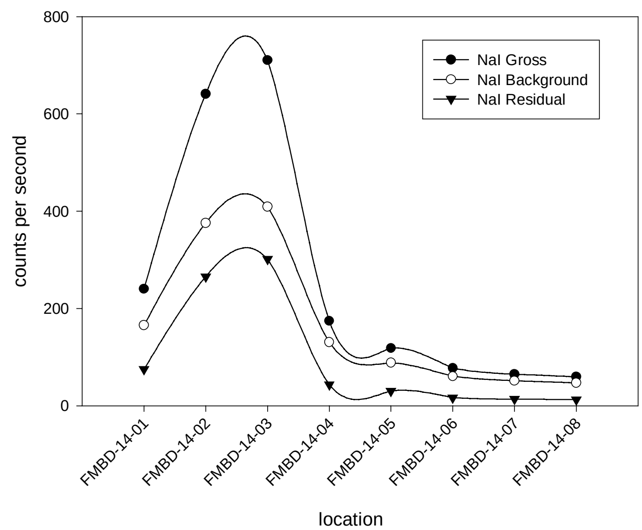

^{137}Cs count rates
FMBD-14, 11/13/01

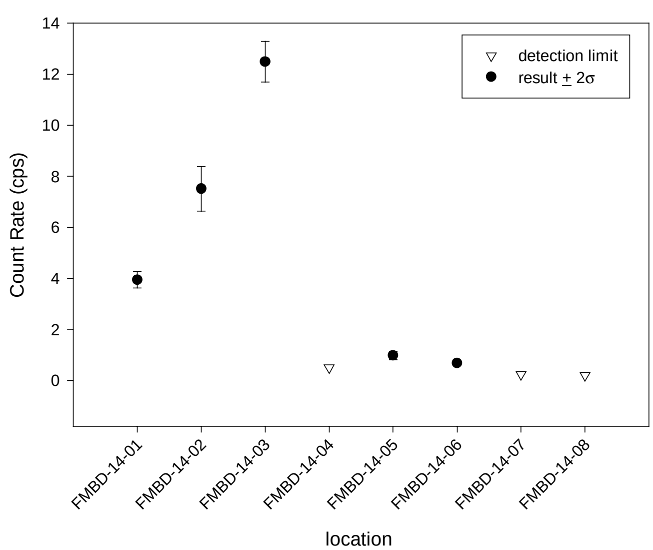

Appendix O: Transect 15

location	residual cps (0-2000 keV)	Cs-137 cps (662 keV)	Cs-137 (pCi/g)	2s error
FMB 15-01	107	3.06	51.8	8.2
FMB 15-02	121	4.20	71.1	7.9
FMB 15-03	148	5.91	100.1	7.8
FMB 15-04	142	4.79	81.2	8.6
FMB 15-05	233	11.47	194.5	11.3
FMB 15-06	249	9.41	159.5	12.2
FMB 15-07	304	10.93	185.3	13.3
FMB 15-08	97	3.43	58.1	8.7
FMB 15-09	125	6.10	103.4	7.0
FMB 15-10	119	3.13	53.0	8.6
FMB 15-11	120	4.46	75.5	6.8

FMBE-015 Transect
11/21/01

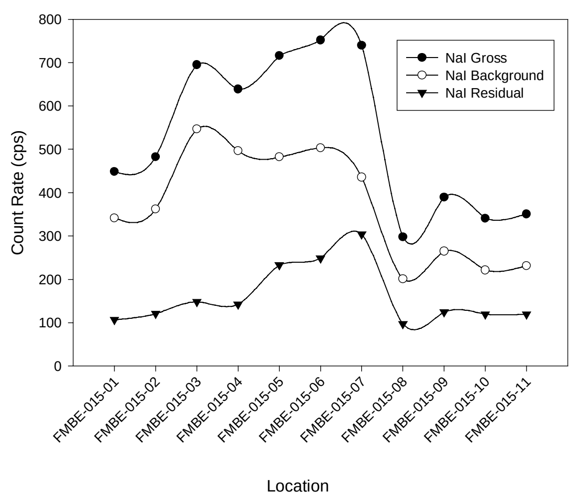

FMBE-015 Transect
^{137}Cs (662 keV)
11/21/01

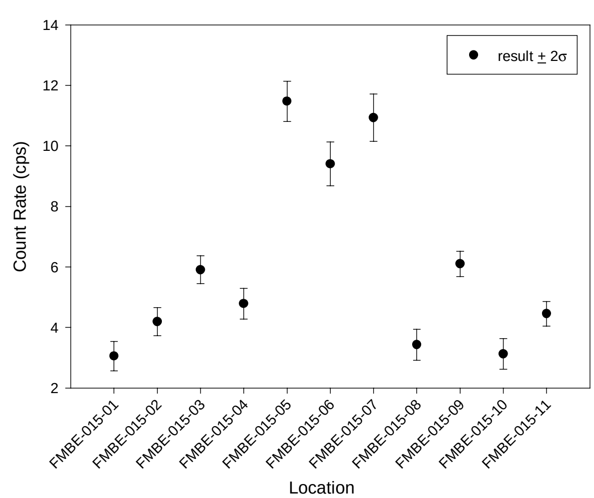

Bore Hole FMBE15-12
^{137}Cs (662 keV) Count Rate
12/6/01

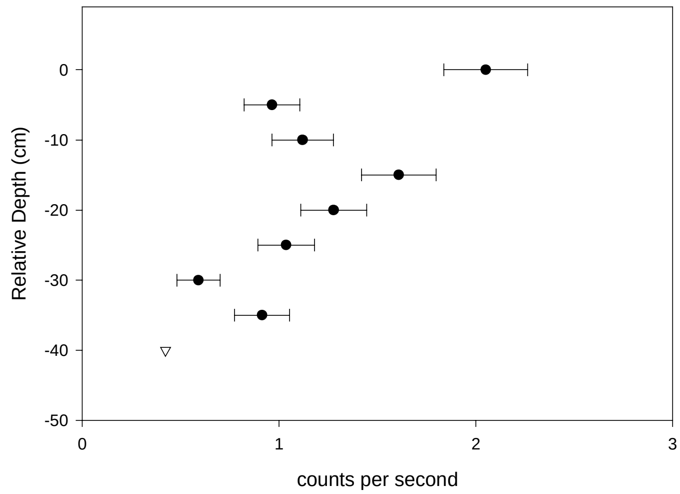

to detector cm	absorber cm	count rate cps	count rate cps	fraction	product
30	0	0.2392	2.1		
35	5	0.1507	1.0	0.128	0.019
40	10	0.0904	1.1	0.149	0.013
45	15	0.0564	1.6	0.214	0.012
50	20	0.04295	1.3	0.170	0.007
55	25	0.02825	1.0	0.138	0.004
60	30	0.01725	0.6	0.079	0.001
65	35	0.01385	0.9	0.122	0.002

total= 7.5 sum= 0.059

Appendix P: Transect 16

location	residual cps (0-2000 keV)	Cs-137 cps (662 keV)	Cs-137 (pCi/g)	2s error
FMB 16-01	124	<0.86	<14.3	
FMB 16-02	147	<0.89	<14.9	
FMB 16-03	87	<0.63	<10.6	
FMB 16-04	44	<0.47	<7.8	
FMB 16-05	84	<0.69	<11.5	
FMB 16-06	47	<0.48	<8.0	
FMB 16-07	44	<0.42	<7.1	
FMB 16-08	81	<0.68	<11.3	
FMB 16-09	20	<0.28	<4.6	
FMB 16-10	58	<0.55	<9.2	

Gross Count Rates
FMBF-16, 11/20/01

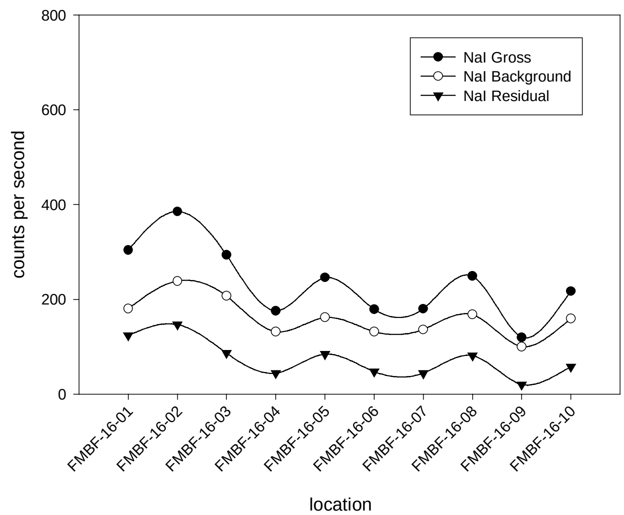

^{137}Cs count rates
FMBF-16, 11/20/01